

Spatio-temporal variability of zooplankton standing stock in
eastern Arabian Sea inferred from ADCP backscatter
measurements

Ranjan Kumar Sahu, D. Shankar, P. Amol, S.G. Aparna, D.V. Desai

November 25, 2024

Abstract

The spatio-temporal variation of zooplankton biomass and standing stock in the eastern Arabian Sea (EAS) is mapped using backscatter measurements from 153.3 kHz acoustic Doppler current profiler (ADCP) moorings deployed at seven locations on the continental slope off the west coast of India from October 2017 to December 2023. The conversion from backscatter to biomass is based on volumetric zooplankton sampling at the respective locations. Analysis of the data over 24–120 m shows that the backscatter and zooplankton biomass decrease from the upper ocean (215 mg^{-3} biomass contour) to the lower depths. Changes are observed in the seasonal variation of the monthly climatology of zooplankton standing stock (integral of the biomass over 24–120 m water column) as we move to poleward along the slope in EAS. The range of variation of standing stock is lowest at Kanyakumari, followed by Okha, which lie at the southern and northern boundary of the EAS,

¹² respectively. While annual cycle is predominant at northeastern Arabian Sea (NEAS), it decreases
¹³ towards southeastern Arabian Sea (SEAS) where the semi-annual cycle tends to dominate. Analysis
¹⁴ reveals weak presence of annual cycle in zooplankton biomass and it is dominated by intraseasonal
¹⁵ and intra-annual components. Intraseasonal variability is often comparable (stronger) to the intra-
¹⁶ annual (annual) variability both of which increases (decreases) poleward with an evident presence in
¹⁷ SEAS. Stronger intraseasonal variability has implication on zooplankton sampling, it's patchiness
¹⁸ and biomass predictability.

₁₉ **1 Introduction**

₂₀ **1.1 Background**

₂₁ Zooplankton plays a vital role in food web of pelagic ecosystem by enabling the hierarchical trans-
₂₂ port of organic matter from primary producers to higher trophic levels impacting the fish population
₂₃ [Ohman and Hirche, 2001] and the carbon pump of the deep ocean [Quéré et al., 2016]. They are
₂₄ presumably the largest migrating organisms in terms of biomass [Hays, 2003] which occurs in diel
₂₅ vertical migration (DVM). Zooplankton depend not only on phytoplankton but other environmen-
₂₆ tal parameters (e.g. mixed layer depth, insolation, oxygen, thermocline, nutrient availability, chl-a
₂₇ (chl-a) concentration and daily primary production). The biological productivity of the ocean is
₂₈ essentially connected with physics and chemistry [Subrahmanyam, 1959, Ryther et al., 1966, Qasim,
₂₉ 1977, Nair, 1970, Banse, 1995, McCreary et al., 2009, Vijith et al., 2016, Amol et al., 2020]. The
₃₀ dynamic ocean results in varying physico-chemical properties, leading to bloom and growth of
₃₁ plankton in favourable conditions. The changes are strongly influenced by the seasonal cycle in the
₃₂ North Indian Ocean (NIO; north of 5 °N of Indian Ocean). The eastern boundary of Arabian Sea
₃₃ contains the West India Coastal Current ([Ramamirtham and Murty, 1965, Banse, 1968, Shetye
₃₄ et al., 1990, McCreary et al., 1993, Amol et al., 2014, Vijith et al., 2016, Chaudhuri et al., 2020,
₃₅ WICC]) which reverses seasonally, flowing poleward (equatorward) during November to February
₃₆ (June to September) ([Shetye et al., 1990, 1991, Vijith et al., 2022]).

₃₇ A direct consequence of this reversal is the seasonal cycle of thermocline ([Prasad and Bahu-
₃₈ layan, 1996, Kumar and Narvekar, 2005]), oxycline ([DeSousa et al., 1996, Schmidt et al., 2020])
₃₉ and thickness of mixed Layer Depth (MLD) ([Shetye et al., 1991, Prasad and Bahulayan, 1996,
₄₀ Kumar and Narvekar, 2005]) induced by upwelling (downwelling) favourable conditions in summer

41 (winter) at eastern Arabian Sea (EAS) facilitated further by wind speed and near-surface stratification. Further, the phytoplankton biomass and chl-a concentration changes with the season
42 [Subrahmanyam and Sarma, 1960, Banse, 1968, Kumar and Narvekar, 2005, Lévy et al., 2007, Vi-
43 jith et al., 2016]. Upwelling in summer monsoon leads to maximum chl-a growth in the entire EAS
44 [Banse, 1968, Banse and English, 2000, McCreary et al., 2009, Hood et al., 2017, Shi and Wang,
45 2022]. During winter monsoon, the convective mixing induced winter mixed layer [Shetye et al.,
46 1992, Madhupratap et al., 1996b, McCreary et al., 1996, Lévy et al., 2007, Shankar et al., 2016,
47 Vijith et al., 2016, Keerthi et al., 2017, Shi and Wang, 2022] results in winter chl-a peak at NEAS
48 while the downwelling Rossby waves modulate chl-a along SEAS albeit limited to coast and islands
49 [Amol et al., 2020].

50 The zooplankton grazing peak is instantaneous with no time delay from peak phytoplankton
51 production [Li et al., 2000, Barber et al., 2001], but its population growth lags [Rehim and Imran,
52 2012, Almén and Tamelander, 2020] depending on its gestation period and other limiting aspects.
53 While some studies suggest that the peak timing of zooplankton may not change in parallel with
54 phytoplankton blooms [Winder and Schindler, 2004], others indicate that lag exists between primary
55 production and the transfer of energy to higher trophic levels [Brock and McClain, 1992, Brock
56 et al., 1991]. The conventional zooplankton measurements, where only few snapshot/s of the event
57 is captured gives an incoherent or incomplete understanding in terms of spatio-temporal variation
58 of zooplankton [Ramamurthy, 1965, Piontkovski et al., 1995, Madhupratap et al., 1992, 1996a,
59 Wishner et al., 1998, Kidwai and Amjad, 2000, Barber et al., 2001, Khandagale et al., 2022] as
60 much information is revealed by later studies [Jyothibabu et al., 2010, Shankar et al., 2019, Aparna
61 et al., 2022] using high resolution data. Calibrated acoustic instruments such as acoustic Doppler
62 current profiler (ADCP) along with relevant data can be utilised to understand small scale variability
63

64 [Nair et al., 1999, Edvardsen et al., 2003, Smith and Madhupratap, 2005, Smeti et al., 2015, Kang
65 et al., 2024], the complex interplay between the physico-chemical parameters and ecosystem [Jiang
66 et al., 2007, Potiris et al., 2018, Shankar et al., 2019, Aparna et al., 2022, Nie et al., 2023], the
67 zooplankton migration [Inoue et al., 2016, Ursella et al., 2018, 2021] and their seasonal to annual
68 variation [Jiang et al., 2007, Hobbs et al., 2021, Liu et al., 2022, Aparna et al., 2022].

69 The relationship between backscatter and the abundance and size of zooplankton was described
70 by Greenlaw [1979] wherein it was pointed out that single frequency backscatter can be used to esti-
71 mate abundance if mean zooplankton size is known. A drastic increase in study temporal and spatial
72 variation of zooplankton biomass using backscatter-proxy came in 1990s by introduction of high
73 frequency echo sounders, with studies [Flagg and Smith, 1989, Wiebe et al., 1990, Batchelder et al.,
74 1995, Greene et al., 1998, Rippeth and Simpson, 1998] methodically showing acoustic backscatter
75 estimated zooplankton biomass. Net sampling augmented ADCP backscatter have been used to
76 study DVM and the spatial and temporal variability of zooplankton biomass in different marine
77 regions, such as the Southwestern Pacific, the Lazarev Sea in Antarctica and the Corsica Channel
78 in the north-western Mediterranean Sea [Cisewski et al., 2010, Hamilton et al., 2013, Smeti et al.,
79 2015, Guerra et al., 2019]. The first such study to exploit the potential of ADCPs in EAS was
80 carried out by Aparna et al. [2022] (A22 from hereon) using ADCP moorings deployed on conti-
81 nental slopes off the Indian west coast. In their work, they showed that the zooplankton standing
82 stock (ZSS) in fact declines during upwelling facilitated increase in phytoplankton biomass. The
83 unusual interaction implies the break down of existing understanding of predator-prey relationship
84 in fundamental level of marine food chain.

85 **1.2 Objective and scope of the manuscript**

86 A network of ADCPs has been installed off the continental slope and shelf on the west coast of
87 India. This ADCPs have enabled a rigorous view of intraseasonal to seasonal scale variability [[Amol](#)
88 [et al., 2014](#), [Chaudhuri et al., 2020](#)] of WICC. In the recent study A22 have used ADCP moorings
89 off Mumbai, Goa and Kollam to explain the temporal variability of zooplankton biomass. The
90 study showed that the zooplankton peaks (and troughs) is not only non-uniform in latitude but
91 also heavily influenced by the oxygen minimum zone, MLD and the seasonal upwelling/downwelling
92 conditions. Stark contrast in the phytoplankton bloom and subsequence growth of zooplankton or
93 the lack thereof was observed in the EAS regimes.

94 We extend the work of A22 by presenting data from four additional moorings in the EAS, show-
95 casing the deviations of seasonal cycle from climatology, and discussing the significant intraseasonal
96 variability of biomass and standing stock revealed by the ADCP data. The paper is organized as
97 follows; datasets and methods employed are described in section 2. Section 3 describes the observed
98 climatology of zooplankton biomass and standing stock. A comparison is drawn to the results of
99 A22. Further, the seasonal cycle of zooplankton biomass and standing stock is discussed with re-
100 lation to the MLD, oxygen, temperature and circulation in determining the biomass is discussed
101 in results section 4. Section 5 delves deeper into the intraseasonal variability with summary and
102 conclusion in section 6.

103 **2 Data and methods**

104 The backscatter data from ADCP and the zooplankton samples collected from the periphery of
105 mooring is described in this section. The backscatter derived from the echo intensity of the seven

106 ADCP mooring deployed on the continental slope off the Indian west coast is the primary data we
107 have use in this manuscript. The moorings details are summarized in [Table 1](#). In situ biomass data
108 from volumetric zooplankton samples are used to validate and correlate with backscatter. The chl-a
109 data is used to study and draw inferences for the possible zooplankton growth seasons. In addition,
110 we have used the monthly climatology of temperature and salinity from [Chatterjee et al. \[2012\]](#).

111 **2.1 ADCP data and backscatter estimation**

112 The ADCPs were deployed on the continental slope off the Indian west coast ([Fig. 1](#)), off Mumbai,
113 Goa, Kollam and Kanyakumari, and later extended to three more sites to cover the entire EAS
114 basin from Okha (22.26°N) in north to Kanyakumari (6.96°N) in south. The other two ADCPs
115 are, 1) Jaigarh at central EAS (CEAS), 2) Udupi (primarily at SEAS regime) in the transition
116 zone between CEAS and SEAS. The extended moorings were deployed in October 2017, though
117 Kanyakumari had been deployed earlier too. However, only Mumbai, Goa and Kollam were part of
118 the previous backscatter study by A22. The moorings are serviced on yearly basis usually during
119 October–November or sometime during September–December (depending on ship availability). The
120 ADCPs are of Teledyne RD Instruments make, upward-looking and operate at 153.3 kHz. While
121 utmost care is taken to position the instrument (mooring) at \sim 150–200 m (\sim 1050–1100 m) depth,
122 yet for some deployments it's shallow or deeper owing to drift caused by floater buoyancy-anchor
123 weight balance. Data was collected at hourly interval and the bin size was set to 4 m. The echoes at
124 surface to 10% range (\sim 20 m) means the data at these depths is rendered useless and is discarded
125 from further use. We have followed the methodology laid down in A22 to derive the backscatter
126 time series from ADCP echo intensity data. The gaps up to two days are filled using the grafting
127 method of [Mukhopadhyay et al. \[2017\]](#) once the zooplankton biomass time series is constructed.

128 **2.2 Zooplankton data and estimation of biomass**

129 The zooplankton samples were collected in the vicinity (~ 10 km) of ADCP mooring site twice,
130 once prior retrieval and again post deployment of moorings so that there is overlap in the ADCP
131 time instance and in situ zooplankton samples during servicing cruises on board of RV Sindhu
132 Sankalp and RV Sindhu Sadhana ([Table 2](#)). Multi-plankton net (MPN) (100 μm mesh size, 0.5 m^2
133 mouth area) was used to get samples in the pre-determined depth ranges; water volume filtered was
134 calculated by the product of sampling depth range and the mouth area of net. The depth range
135 and timing of sample collection was different throughout the MPN hauls (refer [Table 2](#)). From
136 2020 onward, the depth-range was standardized to the bins of 0–25, 25–50, 50–75, 75–100, 100–150
137 (units are in meters). The backscatter obtained earlier is averaged in vertical corresponding to the
138 specific MPN hauls for each site. The backscatter is linearly regressed with respective biomass to
139 establish their relationship ([Fig. 2](#)), which has been demonstrated in numerous previous studies
140 [[Flagg and Smith, 1989](#), [Heywood et al., 1991](#), [Jiang et al., 2007](#), [Aparna et al., 2022](#)].

141 **2.2.1 Biomass time series and estimation of standing stock**

142 The zooplankton biomass time series ([Fig. 3](#)) is created from the above derived linear relationship.
143 The standing stock is determined by taking the depth integral of biomass over the water column.
144 To maintain the consistency of standing stock estimation, only those deployments that doesn't lack
145 data at any depth in the entire range of 24–120 m are considered for analysis as in A22. The lack of
146 data in the above mentioned depth range is due to deviation in positioning of ADCP sensor in the
147 water column. A swift alteration in bathymetry along the continental slope implies that the mooring
148 might anchor at a different depth than planned, hence a change in the predicted position of ADCP.
149 This leads to gap in data at few mooring sites for some year. For example, for the northern-most

150 mooring at Okha, data is not available for the entire upper 120 m depth for the second deployment.
151 Also at Jaigarh, where the surface to ~60 m data (in 3rd deployment) and Kollam, where 80 m
152 and below (in 4th deployment) is unavailable and hence discarded from standing stock estimation.
153 There are few deployments where no or bad data was recorded e.g, at Udupi (4th deployment) and
154 Kanyakumari (6th deployment).

155 **2.3 Mixed-layer depth, temperature, oxygen and chlorophyll**

156 As we are using a 153.3 kHz ADCP moored at ~150 m, the top ~10% of data is unusable because
157 of surface echoes. MLD in EAS is of the order ~20 to 40 m during summer monsoon [Shetye et al.,
158 1990, Shankar et al., 2005, Sreenivas et al., 2008] especially in the SEAS [Shenoi et al., 2005], but
159 during winter the MLD in northern NEAS remains deep [Shankar et al., 2016]. The temperature
160 data is used from Chatterjee et al. [2012], a monthly climatology having 1° spatial resolution.
161 Monthly climatology of oxygen data is obtained from World Ocean Atlas 2013 [García et al., 2014]
162 which contains objectively analyzed 1° climatological fields of in situ measurements. Previous
163 study based on ADCP data of EAS A22 have used SeaWiFS based chl-a data for comparison with
164 climatology of ZSS. The SeaWiFS was at its end of service in 2010, hence we use new chl-a product
165 from Global Ocean Colour, biogeochemical L3 data obtained from [E.U. Copernicus Marine Service](#)
166 [Information](#). The daily data is available at a spatial resolution of 4 km.

167 **3 Time series, climatology and seasonal cycle**

168 A decrease in biomass with increasing depth at all seven study sites is observed ([Fig. 3](#)). To
169 distinguish between high and low productivity zones, we employed a biomass contour, similar
170 to the 215 mg m⁻³ threshold used in A22. However, to better capture seasonal variations off

¹⁷¹ Kanyakumari and Okha, the threshold was replaced by 175 mg m^{-3} . The biomass contour z215
¹⁷² (depth contour D215) and z175 (depth contour D175) allows us to link the seasonal variation
¹⁷³ of biomass to the physico-chemical properties. The monthly climatology of biomass and ZSS is
¹⁷⁴ computed for all locations having valid data in 24–140 m depth range. Climatology of zooplankton
¹⁷⁵ biomass and ZSS is discussed at locations northward starting from southernmost mooring site i.e,
¹⁷⁶ Kanyakumari. Time series, climatology and seasonal cycle of biomass is discussed in the following
¹⁷⁷ subsection 3.2. For a comparison with physico-chemical forcing similar to A22, we use isotherm of
¹⁷⁸ 23°C (henceforth, D23) and oxygen contour specific to each site depending on its position relative
¹⁷⁹ to oxygen minimum zone (OMZ) boundaries of EAS.

¹⁸⁰ 3.1 Time series description

¹⁸¹ Rate of biomass decrease with depth, roughly defined as the difference between mean biomass at
¹⁸² 40 and 104 m depth is highest off Jaigarh and Mumbai as it has higher biomass in upper ocean
¹⁸³ ([Fig. 4 c,b](#)) and lowest off Kanyakumari. This is followed by Goa and Udupi ([Fig. 4 d,e](#)). While
¹⁸⁴ the biomass decrease with depth is lower off Kollam from 2017 to 2020, it becomes considerably
¹⁸⁵ high from thereon ([Fig. 4 f](#)). A comparatively weaker decline in zooplankton biomass with respect
¹⁸⁶ to depth off Okha ([Fig. 3 a1,a2](#)) at NEAS is agreeing with earlier reported data [[Wishner et al., 1998](#),
¹⁸⁷ [Madhupratap et al., 2001](#), [Smith and Madhupratap, 2005](#), [Jyothibabu et al., 2010](#)]. The
¹⁸⁸ sites at SEAS, especially off Kanyakumari and 2017 to 2020 off Kollam also have weaker decrease
¹⁸⁹ [[Madhupratap et al., 2001](#), [Jyothibabu et al., 2010](#), [Aparna et al., 2022](#)]. However, the biomass
¹⁹⁰ decline with depth post 2020 off Kollam is high owing to a strong bloom in these years and is
¹⁹¹ reflected as D215 deepening. D175 and D215 is deep throughout EAS during winter monsoon, but
¹⁹² the occurrence of high biomass is distinct to each regime of EAS. Upper ocean shows considerably

¹⁹³ high biomass and ZSS during winter monsoon at NEAS. On the contrary at SEAS, the upper ocean
¹⁹⁴ shows higher biomass during summer monsoon even though the D215 and D175 is shallower during
¹⁹⁵ this period.

¹⁹⁶ The mean, standard deviation of biomass, ZSS and chl-a are shown in supplementary table
¹⁹⁷ (ST1). A pattern develops from analysis of mean and standard deviation of biomass at 40 and 104
¹⁹⁸ m, with comparatively lower mean biomass off Okha and Goa bifurcated by higher mean biomass
¹⁹⁹ off Mumbai and Jaigarh. Similarly, the lower mean biomass off Udupi and Kanyakumari is divided
²⁰⁰ by higher mean biomass off Kollam. The sites with higher biomass tends to have higher variation
²⁰¹ over time e.g. Mumbai, Jaigarh and Kollam. Variation in the monthly average or seasonal cycle
²⁰² over time suggests presence interannual variability.

²⁰³ 3.2 Climatology of zooplankton biomass and standing stock

²⁰⁴ Off Kanyakumari, z175 is shallower from May onward till October and the zooplankton biomass
²⁰⁵ is comparatively higher than rest of the year ([Fig. 5 g1](#)). The D23 isotherm along-with oxycline
²⁰⁶ (marked by 2.1 ml L^{-1} , a higher oxygen contour as it lies outside OMZ core) follows the same
²⁰⁷ seasonal cycle like D175. However, there is almost no seasonal variation in ZSS off Kanyakumari
²⁰⁸ ($3\sigma, 2.02 \text{ gm m}^{-2}$) as compared to the chl-a variation ($3\sigma, 1.53 \text{ mg m}^{-3}$). At the nearest northern
²⁰⁹ mooring site off Kollam, a strong seasonal cycle is observed and the D215 is deeper for any given
²¹⁰ month. A decline (steep-rise) in ZSS (chl-a biomass) is seen and its minimum (peak) is attained
²¹¹ in August ([Fig. 5 f2](#)). This feature was previously reported by A22, highlighting an imbalance in
²¹² the interaction between zooplankton and phytoplankton. A similar feature is seen further north,
²¹³ off Udupi which sits at the transition zone of SEAS and CEAS, albeit with a relatively weaker zoo-
²¹⁴ plankton biomass and minimum (peak) of ZSS (chl-a) occurring in a month later during September.

215 The D215 seasonal trend off Goa in present study is similar to trend of D215 off Goa as described
216 in A22 (See section xx of supplementary). The biomass off Goa decreases rapidly below the z215
217 as reported earlier, reaching as low as 60 mg m^{-3} at 130 m during June to September (Fig. 5 d1).
218 The ZSS off Jaigarh is identical but stronger to that of off Goa, owing to higher biomass above
219 z215 and the comparatively deeper D215 (Fig. 5 c1). What's intriguing is a presence of strong
220 variation in ZSS off Jaigarh (3σ , 9.72 gm m^{-2}) highest among all locations although the seasonal
221 variation in chl-a biomass (Fig. 5 c2) is visibly non-existent (3σ , 0.15 mg m^{-3}) and lowest among
222 all locations. This is an exact opposite scenario of Kanyakumari, where an insignificant seasonal
223 variation in ZSS is seen even though the chl-a biomass varies strongly. Starting from Kollam (Fig. 5
224 f1) and moving northward to Jaigarh (Fig. 5 c1), we see that the core of high zooplankton biomass
225 gradually shifts from summer (off Kollam) to winter monsoon (off Jaigarh), with the transition of
226 upper ocean zooplankton biomass happening along Udupi and Goa. On the contrary, chl-a biomass
227 tends to have low seasonal range as we move northward from SEAS, with Jaigarh having the least
228 seasonal variation. This shift along with winter monsoon facilitated deeper thermocline leads to an
229 even larger impact on ZSS.

230 Further north off Mumbai the D215 is deeper in December to early April, resulting in a
231 higher ZSS (Fig. 5 b2). D23 follows D215 and the oxycline follows an erratic pattern, reaching
232 depths $> 140 \text{ m}$ during January to March; when a higher biomass is observed above z215. The
233 chl-a biomass shows seasonal variation albeit lower than the SEAS counterpart. At the northern-
234 most site of EAS i.e, off Okha, biomass above z175 is much weaker leading to a relatively lower
235 ZSS (Fig. 5 a1, a2) compared to Mumbai. There's two chl-a peak off Okha, one in February due to
236 convective mixing induced deepening of MLD [Wiggert et al., 2005, Lévy et al., 2007, Keerthi et al.,
237 Shankar et al., 2016] and the other during August in summer monsoon [Wiggert et al., 2005,

²³⁸ Lévy et al., 2007]. The ZSS remains flat during June to September, although the chl-a biomass
²³⁹ increases in this time. Afterwards, ZSS gradually increases and attains its maximum in February
²⁴⁰ same as the chl-a biomass. For a discussion on comparison with A22 climatology, the readers are
²⁴¹ referred to supplementary section xx.

²⁴² 3.3 Seasonal cycle and variability

²⁴³ The deviations from climatology represent the seasonal cycle. This section will deal with a discussion
²⁴⁴ on the seasonal cycle and variability of biomass and ZSS in annual and intra-annual scale along
²⁴⁵ the three regimes of EAS. To understand the variation at a specific period, say 365-days (annual
²⁴⁶ cycle) or 180-days (semi-annual cycle), wavelet analysis is carried out for biomass ([Fig. 6](#)) and ZSS
²⁴⁷ ([Fig. 7](#)). However, if we wish to understand the variation in a specific period band, we use Lanczos
²⁴⁸ filtered time series. A brief discussion on the above mentioned techniques and variability in distinct
²⁴⁹ period band is given in supplementary section xx.

²⁵⁰ From the linear equation correlating biomass and backscatter, the upper and lower bound of
²⁵¹ error limits equals to $\sim 14 \text{ mg m}^{-3}$ ([Fig. 2](#)). The standard deviation incorporating 99.73% data of
²⁵² annual (intra-annual) variability results in its range of 40 mg m^{-3} (80 mg m^{-3}). This higher range
²⁵³ of variability compared to the error range permits us to infer information reliably. However, we
²⁵⁴ are limited by the gaps in time series as discussed in [subsubsection 2.2.1](#). Therefore, we consider
²⁵⁵ locations other than Okha and Jaigarh for the 40 m biomass and ZSS in annual scale.

²⁵⁶ The seasonal cycle is the sum total of annual, semi-annual cycle and their variability. The
²⁵⁷ annual cycle of biomass off Kanyakumari (Udupi and Kollam) is weak (strong), but it varies in
²⁵⁸ time. For example off Kollam, the wavelet power is stronger post 2020 ([Fig. 6](#)). Wavelet analysis of
²⁵⁹ the ZSS time series, derived from integrated biomass between 24 and 120 meters depth, indicates

260 absence (presence) of annual cycle off Kanyakumari (off Udupi) ([Fig. 7 g1](#)). To capture the annual
261 variability, the biomass is passed through Lanczos filter within period of 300 to 400 days ([Fig. 8](#)). The
262 annual variability off Kanyakumari is least among all mooring sites. Kollam shows strong annual
263 variability indicating prominent year-to-year variation of biomass. The intra-annual band ([Fig. 9](#))
264 tends to be stronger compared to the annual band. Much like the annual cycle, the semi-annual
265 cycle is weak and intra-annual variability is moderate off Kanyakumari compared to Kollam and
266 Udupi. However, the strong variability in intra-annual scale is restricted to upper ocean for few
267 years off Kollam.

268 Off Goa, the annual cycle of biomass is comparatively weak contrary to the results of A22,
269 possibly due to shorter time record and low biomass in the recent years as reflected in its ZSS
270 wavelet for 2018 to early 2020 (2021 and 2022) resulting in a weak (strong) annual variability and
271 is also seen in components of biomass variability. Off Goa and Jaigarh, the semi-annual cycle tends
272 to be strong, specifically during 2022 when a anomalous bloom is observed throughout EAS. The
273 semi-annual cycle weakens with depth in these locations. Intra-annual component of seasonal cycle
274 is observed off Goa, with weak (strong) variability during 2019 (2020, 2022) and is moderately
275 strong off Jaigarh. Energy is spread among all intra-annual periods for 2022 off Goa, while during
276 2019 and 2020 the wavelet energy is only present in the semi-annual periods resulting in a overall
277 weaker intra-annual component ([Fig. 6](#)).

278 Further north, a strong annual cycle is seen off Mumbai with strong annual variability highest
279 among EAS sites. Biomass variability in annual scale decreases minutely with depth off Mumbai and
280 the three CEAS sites than off Kollam ([Fig. 8](#)) similar to the observed ocean currents [[Chaudhuri et al., 2020, 2021](#)]. The annual cycle and annual variability of biomass and subsequently, ZSS
282 increases along the slope as we go northward to Mumbai from Kanyakumari. The intra-annual

283 band's strength is reduced off Mumbai and Okha as compared to CEAS and SEAS. The semi-
284 annual cycle is moderately present at 40 m off Mumbai which weakens at 104 m resulting in higher
285 contribution of annual cycle to ZSS. Analysis reveals the presence of moderately strong semi-
286 annual cycle off Okha but only at 104 m and it's intra-annual (annual) band is similar (weaker) in
287 magnitude as compared to Mumbai. Excluding Kanyakumari, intra-annual variability of biomass
288 decreases poleward with higher variation seen off Kollam and Udupi similar to the WICC [[Amol](#)
289 [et al., 2014](#), [Chaudhuri et al., 2020, 2021](#)].

290 4 Intraseasonal variability

291 On the similar lines as discussed in the preceding section, intraseasonal variability of biomass is
292 defined as shifts occurring within a season, typically lasting weeks to months and driven by short-
293 term environmental changes, e.g., nutrient replenishment (depletion) in short-span due to upwelling
294 and/or entrainment (bloom). The variability can be split into two categories; a high-frequency
295 (period < 30 days) and a low-frequency (30 < period < 90 days) component. The presence of
296 significant variation in the 30-day running mean with recurring bursts are seen in the daily data
297 and in the wavelet analysis of biomass at 40 and 104 m ([Fig. 6](#)) lasting few days to a week and
298 distinctive to each location. Most of the spikes in biomass are occurring due to the high-frequency
299 component of intraseasonal band, but our focus is on the low-frequency component seen as bursts
300 lasting much longer than biomass spikes. Much like the intra-annual variability, with a 3σ range of
301 80 mg m^{-3} , meaningful inferences for low-frequency component of intraseasonal variability can be
302 obtained.

303 The strength and contribution of variability components changes over time and differs between
304 EAS regimes as discussed in [subsection 3.3](#). From the wavelet analysis of biomass at 40 and 104

305 m, peaks in low-frequency intraseasonal band is observed across EAS. But the variability can be
306 different at upper and lower regimes at a given location within a specific period band. This differ-
307 ence is evident e.g., during 2019–2021 off Kanyakumari, the wavelet power of biomass within the
308 intraseasonal band declines as we go deeper from 40 m. The filtered biomass in intraseasonal band
309 also showcases the decrease in variability with respect to depth for the same period off Kanyakumari
310 ([Fig. 10](#)). This holds true across EAS with the exception of very few years where the variability
311 at 104 m is comparable or higher than biomass variability at surface layers. However, in other few
312 instances, such as during September–November of 2018 off CEAS, intraseasonal variability remains
313 consistent throughout the entire water column.

314 Strong intraseasonal variability off Kanyakumari relative to the variability in its annual band,
315 along-with comparable or lower range of intra-annual variability ([Fig. 11](#)) and the wavelet at 40 and
316 104 m indicates that the short-lived environmental changes is a major driver of its biomass alongside
317 minor seasonal variation. Off Kollam and Udupi, the presence of intraseasonal bursts is prominent,
318 but due to an equal role of intra-annual component the biomass isn't solely driven by short-term
319 environmental changes. For instance, in 2019 off Kollam ([Fig. 11](#)), intraseasonal variability was
320 dominated by it's high-frequency components. An increase in biomass during the summer monsoon
321 was due to intra-annual and annual variability. However, a sharp decline in August 2019 resulted
322 from reduced intra-annual and intraseasonal variability, even with the presence of a weakly positive
323 annual variability.

324 Off Goa, strong peaks in intraseasonal band is present in wavelet spectra of biomass. However,
325 during early 2019 to late 2020, the intra-annual variability off Goa is non-existent and with the weak
326 annual variability ([Fig. 11](#)), a rather constant biomass at 40 m is observed ([Fig. 4](#)). The wavelet
327 peaks in intraseasonal band occurred strongly in 2018 and later in 2020 during same period, but the

328 absence intra-annual band in 2019 makes it easier to comprehend the contribution of intraseasonal
329 variability. A similar feature is noted off Jaigarh albeit with a weaker magnitude.

330 Weak presence of intraseasonal variability is noticed in the relatively smoother 30-day rolling
331 mean biomass off Mumbai and Okha. During early 2021 off Mumbai, the presence of strong in-
332 traseasonal peaks in wavelet spectra of 104 m along with 40 m shows up in biomass variability in
333 intraseasonal scale ([Fig. 10](#)). Although spectra in the intraseasonal band is present at 40 m off
334 Mumbai and Okha, it is almost absent at 104 m except for a select few years. It implies that the
335 strong variability may occur at deeper depth even when the upper ocean is showing lower variability.
336 Off Okha, the intraseasonal variability is lowest among all EAS sites followed by Mumbai. However,
337 Okha has weak annual and intra-annual variability unlike Mumbai leading to least predictability.

338 The biomass variability at 40 and 104 m in intraseasonal scale is also reflected in the ZSS time
339 series and the corresponding wavelet spectra ([Fig. 7](#)). No annual and semi-annual cycle seems
340 to be present in ZSS off Kanyakumari, but presence of bursts lasting few days to weeks are an
341 indication of intraseasonal variations. While off Kollam and Udupi, the presence of strong intra-
342 annual variations is observed in ZSS alongside intraseasonal variation dominating specifically during
343 September–November. Similarly, off Goa during early 2019 to late 2020 when the intra-annual and
344 annual variations are much weak, strong intraseasonal variation leads to bursts in biomass. However,
345 the strength of intraseasonal variability is reduced at NEAS leading to a comparatively smoother
346 ZSS in 30 day rolling mean window.

347 The intraseasonal peaks in biomass and further ZSS are strong in SEAS followed by CEAS and
348 is weak off NEAS sites. Variability in intraseasonal scale seems to occur predominantly during
349 August to November, for example off Kanyakumari (2018, 2019 and 2020), off Kollam (2018, 2021
350 and 2022) and off Udupi (2018) although it can extend to mid-summer/mid-winter monsoon for

351 few years ([Fig. 10](#)) and is coherent along much of the EAS slope as seen during 2018. The coherence
352 and strong variability at deeper depths at instance (during early 2021 off Mumbai) indicates
353 possible role of ocean circulation in determining biomass at intraseasonal periods. Also, the magnitude
354 of intraseasonal variability of biomass decreases as we move poleward much like the observed
355 intraseasonal currents [[Amol et al., 2014](#), [Chaudhuri et al., 2020, 2021](#)]. However, the strength
356 of intraseasonal variability of biomass is in contrast to the corresponding band of WICC which is
357 strong during winter monsoon along the slope [[Amol et al., 2014](#), [Chaudhuri et al., 2020](#)] and shelf
358 [[Chaudhuri et al., 2021](#)] suggesting further study to identify any possible connection. Nonetheless,
359 the backscatter derived biomass in higher sampling frequency is essential for discussing the low-
360 frequency intraseasonal variability, whereas conventional sampling method such as with research
361 vessel, where one snapshot of biomass is taken in an interval of 15–30 days, would fail to capture
362 these bursts in biomass.

363 5 Discussion

364 5.1 Summary

365 The zooplankton biomass and standing stock across different regions of EAS was examined in this
366 article, highlighting their spatio-temporal trends in the light of physico-chemical parameters using
367 the multi-yearlong ADCP backscatter data from 2017 to 2023.

368 The findings shows notable seasonal variation in zooplankton biomass and ZSS; in SEAS the
369 higher biomass is observed during summer monsoon, while in NEAS the high biomass is observed
370 during winter monsoon with transition of peak biomass happening gradually along CEAS ([subsection 3.2](#)). Off Kollam, a unique double peak in ZSS occurs, one during May to July and another in

372 September to November, suggesting a complex interplay between environmental drivers and zooplankton growth ([Fig. 5 f2](#)). Off Kanyakumari, the seasonal variation in ZSS is non-existent even though a dramatic seasonality is seen in chl-a. On contrary, Jaigarh shows strong variation in ZSS where the chl-a variation is non-existent which could be due to advection owing to presence of WICC. Such feature was observed at bay off Antarctic peninsula and has been attributed to advective influx [[Espinasse et al., 2012](#)]. Climatology shows strong decline in biomass w.r.t. depth off Goa, then NEAS sites off Jaigarh, Mumbai and Okha followed by SEAS locations off Udupi, Kollam and Kanyakumari. The minor peak observed off Mumbai in A22's climatology is absent in the climatology presented using the recent data.

381 Seasonal cycle and variability play a crucial role in regulating biomass. A strong annual cycle is observed at NEAS ([Fig. 6](#)), with biomass peaking during winter monsoon months ([Fig. 5](#)). However, CEAS and SEAS regions particularly off Kollam, exhibit more complex patterns. Off Kollam, the presence of a weak annual cycle and a stronger semi-annual cycle is noted contrary to A22, along with a moderately strong biennial cycle. The semi-annual cycle is especially prominent in the SEAS ([subsection 3.3](#)), where it contributes significantly to the seasonal biomass changes. The variability in annual scale is weak, while that in intra-annual scale is often comparable to intraseasonal variability which is found to influence zooplankton biomass strongly, especially in the summer to winter monsoon transition months ([Fig. 10](#)). The high (low) frequency component of intraseasonal variability determine changes lasting for days (for days to weeks) observed as spikes (bursts) in the daily biomass record ([Fig. 11](#)). Intraseasonal variability is higher in the SEAS, with the NEAS displaying less variance. The intraseasonal variability is often restricted to the upper layer, and it is expected owing to higher variability of chl-a at surface which weakens with increasing depth. The affect of intraseasonal variability compounded with presence of strong intra-

395 annual and weak annual variability is also observed in the difference of mean biomass at 40 and
396 104 m ([Fig. 4](#)). But the variability may exist throughout the water column for few years and can
397 be coherent along the slope suggesting penetration and propagation of intraseasonal scale biomass
398 driver on few occasion.

399 **5.2 consequences of intraseasonal variability**

400 It is evident that the intraseasonal variability dominates the zooplankton biomass along EAS regime
401 ([section 4](#)). A strong intraseasonal component suggests huge implications on sampling, predictabil-
402 ity and zooplankton patchiness.

403 **5.2.1 Implication on sampling**

404 The strength of intraseasonal component changes with time and its magnitude is higher than the
405 other two variabilities ([Fig. 11](#)). In NEAS for example, the SST induced fronts that lasts one to
406 two week ([[Sarma et al., 2018](#), [Sarkar et al., 2019](#)]) can make the region more productive than the
407 surrounding ocean with an increase in integrated chl-a-a ([\[Sarma et al., 2018\]](#)). This could be be
408 potentially leading to the spikes and bursts observed in the daily biomass as seen off Mumbai, Goa
409 and Kollam ([Fig. 11](#)). Strong dependency of zooplankton biomass on the intra-seasonal variation
410 has implication on the sampling of zooplankton using cruises. A servicing cruise along the EAS
411 moorings takes about 12 to 15 days excluding the time to and fro from port to first/last mooring
412 [[Chaudhuri et al., 2020](#), [Aparna et al., 2022](#)]. However, a sampling cruise dedicated to study the
413 spatial variation of zooplankton [[Madhupratap et al., 1992](#), [Smith et al., 1998](#), [Wishner et al., 1998](#),
414 [Kidwai and Amjad, 2000](#)], say for summer monsoon may last a month or more with coarse sampling
415 interval and hence fail to capture the actual biomass within a season for a fair spatial comparison.

⁴¹⁶ One such occasion is a dip in zooplankton biomass off Kollam because of intraseasonal variability
⁴¹⁷ during August, 2019 ([Fig. 11](#)). The resulting biomass is low even though the primary production in
⁴¹⁸ SEAS [[Asha Devi et al., 2010](#), [Jyothibabu et al., 2010](#)] is high and subsequent zooplankton biomass
⁴¹⁹ is supposed to be high.

⁴²⁰ 5.2.2 Zooplankton patchiness

⁴²¹ The species distribution of phytoplankton [[Chowdhury et al., 2021](#)] and further zooplankton in
⁴²² EAS is determined by intricate play based on predation, environment, competition [[Raghukumar](#)
⁴²³ and [Anil, 2003](#)] and hence the forms change [[Madhupratap et al., 1996a](#), [Kidwai and Amjad, 2000](#),
⁴²⁴ [Raghukumar and Anil, 2003](#), [Smith and Madhupratap, 2005](#), [Khandagale et al., 2022](#)], with few
⁴²⁵ species dominating in certain seasons. Habitat patchiness, i.e, irregular distribution of habitats
⁴²⁶ and resources in the deep-sea environment [[Egginton et al., 1998](#), [Raghukumar and Anil, 2003](#)]
⁴²⁷ contributes to high biodiversity which in turn can affect ecosystem dynamics. A high intraseasonal
⁴²⁸ variability in zooplankton biomass suggests that patchiness in the deep-sea environment isn't solely
⁴²⁹ driven by seasonal cycles but also occurs within individual seasons. Carefully planned sampling of
⁴³⁰ zooplankton with low intervals is necessary to access the zooplankton patchiness within a season.

⁴³¹ 5.2.3 Predictability

⁴³² Though EAS shows a strong seasonal cycle of current, there are notable differences between regimes
⁴³³ of EAS. Kollam's seasonal cycle is marked by intense intraseasonal bursts making the shelf WICC
⁴³⁴ at Kollam highly unpredictable [[Chaudhuri et al., 2021](#)] and the intraseasonal variability increases
⁴³⁵ equatorward. The direction of WICC at any given time of the year can be either poleward or equa-
⁴³⁶ torward owing to the bursts. Assuming that advection and entrainment can influence zooplankton
⁴³⁷ forms and since the annual variation of biomass is much weaker, current driven intraseasonal vari-

438 ations of biomass in rather unpredictable manner is expected. The zooplankton biomass varies
439 frequently and strongly within the season itself ([section 4](#)). This intraseasonal variability indicates
440 that zooplankton populations and their patches fluctuate due to short-term changes, likely respond-
441 ing to factors like temperature shifts, food availability, or ocean environment. So, the zooplankton
442 biomass much like the current is dominated by intraseasonal variations more than the annual cycle.

443 Finding similarity in the trend of increasing (decreasing) intraseasonal and intra-annual (annual)
444 variability of biomass and currents as we go equatorward along the EAS slope is tempting, as it
445 indicates a link between the two. However, a rigorous study is necessary to indicate any such
446 relationship. On similar note, the inter-annual variability of chl-a is less in comparison to its seasonal
447 variability [[Shi and Wang, 2022](#)] much like the zooplankton. Strong peaks in intraseasonal band
448 in chl-a was evident in Lomb–Scargle periodogram (figure not shown), analogous to zooplankton
449 biomass and ZSS, but lacked concrete evidence of direct correlation.

450 5.3 Conclusion

451 The results presented in this paper are based on the ADCP backscatter which is suitable for creating
452 long-term time series of zooplankton biomass in open ocean. Along-with the physico-chemical
453 drivers for seasonal and further the climatological cycle of biomass, we provided evidence of strong
454 intraseasonal variation. Possible role of circulation in determining biomass was indicative from the
455 analysis. Although, it wasn't studied in the present work, the current data from ADCPs provide
456 additional advantage of exploring the link with circulation. There are however, certain limitations
457 to approach of studying biomass using ADCP backscatter. While the variation in depth is captured
458 with in situ samples from MPN, the variation in season is not adequately addressed owing to the
459 limitation of months when ADCP servicing cruises are undertaken apart from availability. The west

460 coast cruises for ADCP servicing are planned for the monsoon transition months but may start as
461 early as late September till December with few exceptions such as 2022 when it was carried out
462 in March. Since the intraseasonal and intra-annual variability is almost double that of the annual
463 one ([section 4](#)), the sampling done in particular season for biomass-backscatter comparison isn't
464 sufficient. For a better approach to capture the seasonal variation, more in situ samples are needed
465 from the less explored seasons.

466 While we are able to infer the biomass information, any information regarding the size distribu-
467 tion of zooplankton and their contribution to ZSS is lost. In western Arabian sea, microzooplank-
468 ton dominated the grazing processes by consuming approximately 71% of the primary production
469 [[Reckermann and Veldhuis, 1997](#), [Marra and Barber, 2005](#), [Landry, 2009](#)]. Mesozooplankton, in
470 turn relied on microzooplankton for about 40% of their food [[Landry, 2009](#), [Hood et al., 2024](#)].
471 However, the relative grazing importance of micro and mesozooplankton fluctuated seasonally and
472 spatially, affecting the overall impact on phytoplankton biomass in a way that aligns with the theory
473 of grazing control or trophic cascade [[Ripple et al., 2016](#)] in the Arabian Sea [[Marra and Barber,](#)
474 [2005](#), [Landry, 2009](#)]. To understand the intricate complexities of different forms of meso- and mi-
475 crozooplankton and their interaction, a robust multi-frequency, size-resolving backscatter data can
476 be utilised. However, a mono-frequency ADCP is adequately suitable to capture the intraseasonal
477 variation of zooplankton that will otherwise be left inaccessible by conventional sampling means.

478 6 Declaration of competing interest

479 The authors declare that they have no known competing financial interests or personal relationships
480 that could have appeared to influence the work reported in this paper.

481 **7 Acknowledgments**

482 The data were collected by xxx with fund provided under xxxx. The mooring programme is
483 supported by INCOIS (Indian National Centre for Ocean Information Services, Hyderabad) and
484 CSIR. We acknowledge the contribution of mooring division and ship cell of CSIR-NIO.

485 Ranjan Kumar Sahu expresses his acknowledgment to the Council of Scientific and Industrial
486 Research (CSIR) for sponsoring his fellowship. Additionally, he extends his thanks to Ashok
487 Kankonkar for providing the essential data, Rahul Khedekar for his data processing, Roshan D'Souza
488 for his diligent work in biological data analysis. Their contributions were invaluable to the successful
489 completion of this research.

490 **References**

- 491 Anna-Karin Almén and Tobias Tamelander. Temperature-related timing of the spring bloom and match between
492 phytoplankton and zooplankton. *Marine Biology Research*, 16(8-9):674–682, 2020.
- 493 P Amol, D Shankar, V Fernando, A Mukherjee, SG Aparna, R Fernandes, GS Michael, ST Khalap, NP Satelkar,
494 Y Agarvadekar, et al. Observed intraseasonal and seasonal variability of the west india coastal current on the
495 continental slope. *Journal of Earth System Science*, 123(5):1045–1074, 2014.
- 496 P Amol, Suchandan Bemal, D Shankar, V Jain, V Thushara, V Vijith, and PN Vinayachandran. Modulation of
497 chlorophyll concentration by downwelling rossby waves during the winter monsoon in the southeastern arabian
498 sea. *Progress in Oceanography*, 186:102365, 2020.
- 499 SG Aparna, DV Desai, D Shankar, AC Anil, Shrikant Dora, and R Khedekar. Seasonal cycle of zooplankton standing
500 stock inferred from adcp backscatter measurements in the eastern arabian sea. *Progress in Oceanography*, 203:
501 102766, 2022.
- 502 C.R. Asha Devi, R. Jyothibabu, P. Sabu, Josia Jacob, H. Habeebrehman, M.P. Prabhakaran, K.J. Jayalakshmi, and
503 C.T. Achuthankutty. Seasonal variations and trophic ecology of microzooplankton in the southeastern arabian
504 sea. *Continental Shelf Research*, 30(9):1070–1084, 2010. ISSN 0278-4343. doi: <https://doi.org/10.1016/j.csr.2010.02.007>. URL <https://www.sciencedirect.com/science/article/pii/S0278434310000439>.
- 506 K Banse and DC English. Geographical differences in seasonality of czcs-derived phytoplankton pigment in the
507 arabian sea for 1978–1986. *Deep Sea Research Part II: Topical Studies in Oceanography*, 47(7-8):1623–1677, 2000.

- 508 Karl Banse. Hydrography of the arabian sea shelf of india and pakistan and effects on demersal fishes. In *Deep sea*
509 *research and oceanographic Abstracts*, volume 15, pages 45–79. Elsevier, 1968.
- 510 Karl Banse. Zooplankton: pivotal role in the control of ocean production: I. biomass and production. *ICES Journal*
511 *of marine Science*, 52(3-4):265–277, 1995.
- 512 Richard T Barber, John Marra, Robert C Bidigare, Louis A Codispoti, David Halpern, Zackary Johnson, Mikel
513 Latasa, Ralf Goericke, and Sharon L Smith. Primary productivity and its regulation in the arabian sea during
514 1995. *Deep Sea Res. Part 2 Top. Stud. Oceanogr.*, 48(6-7):1127–1172, jan 2001.
- 515 H. P. Batchelder, J. R. VanKeuren, R. D. Vaillancourt, and E. Swift. Spatial and temporal distributions of acoustically
516 estimated zooplankton biomass near the marine light-mixed layers station ($59^{\circ}30'N$, $21^{\circ}00'W$) in the north atlantic
517 in may 1991. *Journal of Geophysical Research: Oceans*, 100:6549–6563, 1995. doi: 10.1029/94jc00981.
- 518 John C Brock and Charles R McClain. Interannual variability in phytoplankton blooms observed in the northwestern
519 arabian sea during the southwest monsoon. *Journal of Geophysical Research: Oceans*, 97(C1):733–750, 1992.
- 520 John C Brock, Charles R McClain, Mark E Luther, and William W Hay. The phytoplankton bloom in the north-
521 western arabian sea during the southwest monsoon of 1979. *Journal of Geophysical Research: Oceans*, 96(C11):
522 20623–20642, 1991.
- 523 Abhisek Chatterjee, D Shankar, SSC Shenoi, GV Reddy, GS Michael, M Ravichandran, VV Gopalkrishna,
524 EP Rama Rao, TVS Udaya Bhaskar, and VN Sanjeevan. A new atlas of temperature and salinity for the north
525 indian ocean. *Journal of Earth System Science*, 121:559–593, 2012.
- 526 Anya Chaudhuri, D Shankar, SG Aparna, P Amol, V Fernando, A Kankonkar, GS Michael, NP Satelkar, ST Khalap,
527 AP Tari, et al. Observed variability of the west india coastal current on the continental slope from 2009–2018.
528 *Journal of Earth System Science*, 129(1):57, 2020.
- 529 Anya Chaudhuri, P Amol, D Shankar, S Mukhopadhyay, SG Aparna, V Fernando, and A Kankonkar. Observed
530 variability of the west india coastal current on the continental shelf from 2010–2017. *Journal of Earth System
531 Science*, 130:1–21, 2021.
- 532 Mintu Chowdhury, Haimanti Biswas, Aditi Mitra, Saumya Silori, Diksha Sharma, Debasmita Bandyopadhyay, Aziz
533 Ur Rahman Shaik, Veronica Fernandes, and Jayu Narvekar. Southwest monsoon-driven changes in the phyto-
534 plankton community structure in the central arabian sea (2017–2018): After two decades of jgofs. *Progress in
535 Oceanography*, 197:102654, 2021.
- 536 Boris Cisewski, Volker H Strass, Monika Rhein, and Sören Krägesky. Seasonal variation of diel vertical migration
537 of zooplankton from adcp backscatter time series data in the lazarev sea, antarctica. *Deep Sea Research Part I:
538 Oceanographic Research Papers*, 57(1):78–94, 2010.
- 539 Kent L Deines. Backscatter estimation using broadband acoustic doppler current profilers. In *Proceedings of the
540 IEEE Sixth Working Conference on Current Measurement (Cat. No. 99CH36331)*, pages 249–253. IEEE, 1999.

- 541 SN DeSousa, M Dileepkumar, S Sardessai, VVSS Sarma, and PV Shirodkar. Seasonal variability in oxygen and
542 nutrients in the central and eastern arabian sea. Indian Academy of Sciences, 1996.
- 543 A Edvardsen, D Slagstad, KS Tande, and P Jaccard. Assessing zooplankton advection in the barents sea using
544 underway measurements and modelling. *Fisheries Oceanography*, 12(2):61–74, 2003.
- 545 David B Eggleston, Lisa L Etherington, and Ward E Elis. Organism response to habitat patchiness: species and
546 habitat-dependent recruitment of decapod crustaceans. *Journal of experimental marine biology and ecology*, 223
547 (1):111–132, 1998.
- 548 Boris Espinasse, Meng Zhou, Yiwu Zhu, Elliott L Hazen, Ari S Friedlaender, Douglas P Nowacek, Dezhang Chu,
549 and Francois Carlotti. Austral fall- winter transition of mesozooplankton assemblages and krill aggregations in an
550 embayment west of the antarctic peninsula. *Marine Ecology Progress Series*, 452:63–80, 2012.
- 551 Charles N Flagg and Sharon L Smith. On the use of the acoustic doppler current profiler to measure zooplankton
552 abundance. *Deep Sea Research Part A. Oceanographic Research Papers*, 36(3):455–474, 1989.
- 553 H. E. García, R. A. Locarnini, T. P. Boyer, J. I. Antonov, A. V. Mishonov, O. K. Baranova, M. M. Zweng, J. R.
554 Reagan, and D. R. Johnson. Dissolved oxygen, apparent oxygen utilization, and oxygen saturation. *NOAA Atlas
555 NESDIS 75*, 3, 2014.
- 556 Charles H Greene, Peter H Wiebe, Chris Pelkie, Mark C Benfield, and Jacqueline M Popp. Three-dimensional
557 acoustic visualization of zooplankton patchiness. *Deep Sea Research Part II: Topical Studies in Oceanography*, 45
558 (7):1201–1217, 1998.
- 559 Charles F Greenlaw. Acoustical estimation of zooplankton populations 1. *Limnology and Oceanography*, 24(2):
560 226–242, 1979.
- 561 Davide Guerra, Katrin Schroeder, Mireno Borghini, Elisa Camatti, Marco Pansera, Anna Schroeder, Stefania
562 Sparnocchia, and Jacopo Chiggiato. Zooplankton diel vertical migration in the corsica channel (north-western
563 mediterranean sea) detected by a moored acoustic doppler current profiler. *Ocean Science*, 15(3):631–649, 2019.
- 564 James M Hamilton, Kate Collins, and Simon J Prinsenberg. Links between ocean properties, ice cover, and plankton
565 dynamics on interannual time scales in the canadian arctic archipelago. *Journal of Geophysical Research: Oceans*,
566 118(10):5625–5639, 2013.
- 567 Graeme C Hays. A review of the adaptive significance and ecosystem consequences of zooplankton diel vertical
568 migrations. In *Migrations and Dispersal of Marine Organisms: Proceedings of the 37 th European Marine Biology
569 Symposium held in Reykjavík, Iceland, 5–9 August 2002*, pages 163–170. Springer, 2003.
- 570 Karen J Heywood, S Scrope-Howe, and ED Barton. Estimation of zooplankton abundance from shipborne adcp
571 backscatter. *Deep Sea Research Part A. Oceanographic Research Papers*, 38(6):677–691, 1991.

- 572 Laura Hobbs, Neil S Banas, Jonathan H Cohen, Finlo R Cottier, Jørgen Berge, and Øystein Varpe. A marine
573 zooplankton community vertically structured by light across diel to interannual timescales. *Biology Letters*, 17(2):
574 20200810, 2021.
- 575 Raleigh R Hood, Lynnath E Beckley, and Jerry D Wiggert. Biogeochemical and ecological impacts of boundary
576 currents in the indian ocean. *Progress in Oceanography*, 156:290–325, 2017.
- 577 Raleigh R Hood, Victoria J Coles, Jenny A Huggett, Michael R Landry, Marina Levy, James W Moffett, and Timothy
578 Rixen. Nutrient, phytoplankton, and zooplankton variability in the indian ocean. In *The Indian Ocean and its*
579 *role in the global climate system*, pages 293–327. Elsevier, 2024.
- 580 Ryuichiro Inoue, Minoru Kitamura, and Tetsuichi Fujiki. Diel vertical migration of zooplankton at the s 1 biogeo-
581 chemical mooring revealed from acoustic backscattering strength. *Journal of Geophysical Research: Oceans*, 121
582 (2):1031–1050, 2016.
- 583 Songnian Jiang, Tommy D Dickey, Deborah K Steinberg, and Laurence P Madin. Temporal variability of zooplankton
584 biomass from adcp backscatter time series data at the bermuda testbed mooring site. *Deep Sea Research Part I:*
585 *Oceanographic Research Papers*, 54(4):608–636, 2007.
- 586 R Jyothibabu, NV Madhu, H Habeebrehman, KV Jayalakshmy, KKC Nair, and CT Achuthankutty. Re-evaluation
587 of ‘paradox of mesozooplankton’ in the eastern arabian sea based on ship and satellite observations. *Journal of*
588 *Marine Systems*, 81(3):235–251, 2010.
- 589 Myounghee Kang, Sunyoung Oh, Wooseok Oh, Dong-Jin Kang, SungHyun Nam, and Kyoungsoon Lee. Acoustic
590 characterization of fish and macroplankton communities in the seychelles-chagos thermocline ridge of the southwest
591 indian ocean. *Deep Sea Research Part II: Topical Studies in Oceanography*, 213:105356, 2024.
- 592 Madhavan Girijakumari Keerthi, Matthieu Lengaigne, Marina Levy, Jerome Vialard, Vallivattathillam Parvathi,
593 Clément de Boyer Montégut, Christian Ethé, Olivier Aumont, Iyyappan Suresh, Valiya Parambil Akhil, et al.
594 Physical control of interannual variations of the winter chlorophyll bloom in the northern arabian sea. *Biogeosciences*, 14(15):3615–3632, 2017.
- 596 Punam A Khandagale, Vaibhav D Mhatre, and Sujitha Thomas. Seasonal and spatial variability of zooplankton
597 diversity in north eastern arabian sea along the maharashtra coast. *Journal of the Marine Biological Association*
598 *of India*, 64(1):25–32, 2022.
- 599 S Kidwai and S Amjad. Zooplankton: pre-southwest and northeast monsoons of 1993 to 1994, from the north arabian
600 sea. *Mar. Biol.*, 136(3):561–571, apr 2000.
- 601 S. Prasanna Kumar and Jayu Narvekar. Seasonal variability of the mixed layer in the central arabian sea and its
602 implication on nutrients and primary productivity. *Deep Sea Research Part II: Topical Studies in Oceanography*,
603 52(14):1848–1861, 2005. ISSN 0967-0645. doi: <https://doi.org/10.1016/j.dsr2.2005.06.002>. URL <https://www.sciencedirect.com/science/article/pii/S0967064505001207>. Biogeochemical Processes in the Northern Indian
604 Ocean.

- 606 Michael R Landry. Grazing processes and secondary production in the arabian sea: A simple food web synthesis
607 with measurement constraints. In *Indian Ocean Biogeochemical Processes and Ecological Variability*, Geophysical
608 monograph, pages 133–146. American Geophysical Union, Washington, D. C., 2009.
- 609 Marina Lévy, D Shankar, J-M André, SSC Shenoi, Fabien Durand, and Clément de Boyer Montégut. Basin-wide
610 seasonal evolution of the indian ocean's phytoplankton blooms. *Journal of Geophysical Research: Oceans*, 112
611 (C12), 2007.
- 612 M Li, A Gargett, and K Denman. What determines seasonal and interannual variability of phytoplankton and
613 zooplankton in strongly estuarine systems? *Estuarine, Coastal and Shelf Science*, 50(4):467–488, 2000.
- 614 Yanliang Liu, Jingsong Guo, Yuhuan Xue, Chalermrat Sangmanee, Huiwu Wang, Chang Zhao, Somkiat Khokiat-
615 tiwong, and Weidong Yu. Seasonal variation in diel vertical migration of zooplankton and micronekton in the
616 andaman sea observed by a moored adcp. *Deep Sea Research Part I: Oceanographic Research Papers*, 179:103663,
617 2022.
- 618 M Madhupratap, P Haridas, Neelam Ramaiah, and CT Achuthankutty. Zooplankton of the southwest coast of india:
619 abundance, composition, temporal and spatial variability in 1987. 1992.
- 620 M Madhupratap, TC Gopalakrishnan, P Haridas, KKC Nair, PN Aravindakshan, G Padmavati, and Shiney Paul.
621 Lack of seasonal and geographic variation in mesozooplankton biomass in the arabian sea and its structure in the
622 mixed layer. *Current science. Bangalore*, 71(11):863–868, 1996a.
- 623 M Madhupratap, S Prasanna Kumar, PMA Bhattathiri, M Dileep Kumar, S Raghukumar, KKC Nair, and N Rama-
624 iah. Mechanism of the biological response to winter cooling in the northeastern arabian sea. *Nature*, 384(6609):
625 549–552, 1996b.
- 626 M Madhupratap, TC Gopalakrishnan, P Haridas, and KKC Nair. Mesozooplankton biomass, composition and
627 distribution in the arabian sea during the fall intermonsoon: implications of oxygen gradients. *Deep Sea Research
628 Part II: Topical Studies in Oceanography*, 48(6-7):1345–1368, 2001.
- 629 John Marra and Richard T. Barber. Primary productivity in the arabian sea: A synthesis of jgofs data. *Progress
630 in Oceanography*, 65(2):159–175, 2005. ISSN 0079-6611. doi: <https://doi.org/10.1016/j.pocean.2005.03.004>. URL
631 <https://www.sciencedirect.com/science/article/pii/S007966110500042X>. The Arabian Sea of the 1990s: New
632 Biogeochemical Understanding.
- 633 JP McCreary, Raghu Murtugudde, Jerome Vialard, PN Vinayachandran, Jerry D Wiggert, Raleigh R Hood,
634 D Shankar, and S Shetye. Biophysical processes in the indian ocean. *Indian Ocean biogeochemical processes
635 and ecological variability*, 185:9–32, 2009.
- 636 Julian P McCreary, Pijush K Kundu, and Robert L Molinari. A numerical investigation of dynamics, thermodynamics
637 and mixed-layer processes in the indian ocean. *Progress in Oceanography*, 31(3):181–244, 1993.
- 638 Julian P McCreary, Kevin E Kohler, Raleigh R Hood, and Donald B Olson. A four-component ecosystem model of
639 biological activity in the arabian sea. *Progress in Oceanography*, 37(3-4):193–240, 1996.

- 640 S Mukhopadhyay, D Shankar, S G Aparna, and A Mukherjee. Observations of the sub-inertial, near-surface east
641 india coastal current. *Cont. Shelf Res.*, 148:159–177, September 2017.
- 642 KKC Nair, M Madhupratap, TC Gopalakrishnan, P Haridas, and Mangesh Gauns. The arabian sea: physical
643 environment, zooplankton and myctophid abundance. 1999.
- 644 PV Nair. Primary productivity in the indian seas. *CMFRI Bulletin*, 22:1–63, 1970.
- 645 Lingyun Nie, Jianchao Li, Hao Wu, Wenchao Zhang, Yongjun Tian, Yang Liu, Peng Sun, Zhenjiang Ye, Shuyang
646 Ma, and Qinfeng Gao. The influence of ocean processes on fine-scale changes in the yellow sea cold water mass
647 boundary area structure based on acoustic observations. *Remote Sensing*, 15(17):4272, 2023.
- 648 MD Ohman and H-J Hirche. Density-dependent mortality in an oceanic copepod population. *Nature*, 412(6847):
649 638–641, 2001.
- 650 SA Piontkovski, R Williams, and TA Melnik. Spatial heterogeneity, biomass and size structure of plankton of the
651 indian ocean: some general trends. *Marine ecology progress series*, pages 219–227, 1995.
- 652 Emmanuel Potiris, Constantin Frangoulis, Alkiviadis Kalampokis, Manolis Ntoumas, Manos Pettas, George Peti-
653 hakis, and Vassilis Zervakis. Acoustic doppler current profiler observations of migration patterns of zooplankton
654 in the cretan sea. *Ocean Science*, 14(4):783–800, 2018.
- 655 TG Prasad and N Bahulayan. Mixed layer depth and thermocline climatology of the arabian sea and western
656 equatorial indian ocean. 1996.
- 657 SZ Qasim. Biological productivity of the indian ocean. 1977.
- 658 Corinne Le Quéré, Robbie M Andrew, Josep G Canadell, Stephen Sitch, Jan Ivar Korsbakken, Glen P Peters,
659 Andrew C Manning, Thomas A Boden, Pieter P Tans, Richard A Houghton, et al. Global carbon budget 2016.
660 *Earth System Science Data*, 8(2):605–649, 2016.
- 661 Seshagiri Raghukumar and AC Anil. Marine biodiversity and ecosystem functioning: A perspective. *Current Science*,
662 84(7):884–892, 2003.
- 663 CP Ramamirtham and AVS Murty. Hydrography of the west coast of india during the pre-monsoon period of the
664 year 1962—part 2: in and offshore waters of the konkan and malabar coasts. *Journal of the Marine Biological
665 Association of India*, 7(1):150–168, 1965.
- 666 S Ramamurthy. Studies on the plankton of the north kanara coast in relation to the pelagic fishery. *Journal of
667 Marine Biological Association of India*, 7(1):127–149, 1965.
- 668 M Reckermann and M J W Veldhuis. Trophic interactions between picophytoplankton and micro- and nanozoo-
669 plankton in the western arabian sea during the NE monsoon 1993. *Aquat. Microb. Ecol.*, 12:263–273, 1997.
- 670 Mehbuba Rehim and Mudassar Imran. Dynamical analysis of a delay model of phytoplankton–zooplankton interac-
671 tion. *Applied Mathematical Modelling*, 36(2):638–647, 2012.

- 672 T. P. Rippeth and J. H. Simpson. Diurnal signals in vertical motions on the hebridean shelf. *Limnology and*
673 *Oceanography*, 43:1690–1696, 1998. doi: 10.4319/lo.1998.43.7.1690.
- 674 William J Ripple, James A Estes, Oswald J Schmitz, Vanessa Constant, Matthew J Kaylor, Adam Lenz, Jennifer L
675 Motley, Katharine E Self, David S Taylor, and Christopher Wolf. What is a trophic cascade? *Trends Ecol. Evol.*,
676 31(11):842–849, November 2016.
- 677 John H Ryther, John R Hall, Allan K Pease, Andrew Bakun, and Mark M Jones. Primary organic production in
678 relation to the chemistry and hydrography of the western indian ocean 1. *Limnology and Oceanography*, 11(3):
679 371–380, 1966.
- 680 Kankan Sarkar, SG Aparna, Shrikant Dora, and D Shankar. Seasonal variability of sea-surface temperature fronts
681 associated with large marine ecosystems in the north indian ocean. *Journal of Earth System Science*, 128(1):20,
682 2019.
- 683 VVSS Sarma, DV Desai, JS Patil, L Khandeparker, SG Aparna, D Shankar, Selrina D'Souza, HB Dalabehera,
684 J Mukherjee, P Sudharani, et al. Ecosystem response in temperature fronts in the northeastern arabian sea.
685 *Progress in Oceanography*, 165:317–331, 2018.
- 686 Henrike Schmidt, Rena Czeschel, and Martin Visbeck. Seasonal variability of the arabian sea intermediate circulation
687 and its impact on seasonal changes of the upper oxygen minimum zone. *Ocean Science*, 16(6):1459–1474, 2020.
- 688 D Shankar, SSC Shenoi, RK Nayak, PN Vinayachandran, G Nampoothiri, AM Almeida, GS Michael, MR Ramesh
689 Kumar, D Sundar, and OP Sreejith. Hydrography of the eastern arabian sea during summer monsoon 2002.
690 *Journal of earth system science*, 114:459–474, 2005.
- 691 D Shankar, R Remya, PN Vinayachandran, Abhisek Chatterjee, and Ambica Behera. Inhibition of mixed-layer
692 deepening during winter in the northeastern arabian sea by the west india coastal current. *Climate Dynamics*,
693 47:1049–1072, 2016.
- 694 D Shankar, R Remya, AC Anil, and V Vijith. Role of physical processes in determining the nature of fisheries in the
695 eastern arabian sea. *Progress in Oceanography*, 172:124–158, 2019.
- 696 SSC Shenoi, D Shankar, GS Michael, J Kurian, KK Varma, MR Ramesh Kumar, AM Almeida, AS Unnikrishnan,
697 W Fernandes, N Barreto, et al. Hydrography and water masses in the southeastern arabian sea during march–june
698 2003. *Journal of earth system science*, 114:475–491, 2005.
- 699 SR Shetye, AD Gouveia, SSC Shenoi, D Sundar, GS Michael, AM Almeida, and K Santanam. Hydrography and
700 circulation off the west coast of india during the southwest monsoon 1987. 1990.
- 701 S.R. Shetye, A.D. Gouveia, S.S.C. Shenoi, G.S. Michael, D. Sundar, A.M. Almeida, and K. Santanam. The coastal
702 current off western india during the northeast monsoon. *Deep Sea Research Part A. Oceanographic Research*
703 *Papers*, 38(12):1517–1529, 1991. ISSN 0198-0149. doi: [https://doi.org/10.1016/0198-0149\(91\)90087-V](https://doi.org/10.1016/0198-0149(91)90087-V). URL
704 <https://www.sciencedirect.com/science/article/pii/019801499190087V>.

- 705 SR Shetye, AD Gouveia, and SSC Shenoi. Does winter cooling lead to the subsurface salinity minimum off saurashtra,
706 india? *Oceanography of the Indian Ocean*, pages 617–625, 1992.
- 707 Wei Shi and Menghua Wang. Phytoplankton biomass dynamics in the arabian sea from viirs observations. *Journal
708 of Marine Systems*, 227:103670, 2022.
- 709 Houssem Smeti, Marc Pagano, Christophe Menkes, Anne Lebourges-Dhaussy, Brian PV Hunt, Valerie Allain, Martine
710 Rodier, Florian De Boissieu, Elodie Kestenare, and Cherif Sammari. Spatial and temporal variability of zooplank-
711 ton off n ew c aledonia (s outhwestern p acific) from acoustics and net measurements. *Journal of Geophysical
712 Research: Oceans*, 120(4):2676–2700, 2015.
- 713 Sharon Smith, Michael Roman, Irina Prusova, Karen Wishner, Marcia Gowing, LA Codispoti, Richard Barber, John
714 Marra, and Charles Flagg. Seasonal response of zooplankton to monsoonal reversals in the arabian sea. *Deep Sea
715 Research Part II: Topical Studies in Oceanography*, 45(10-11):2369–2403, 1998.
- 716 SL Smith and M Madhupratap. Mesozooplankton of the arabian sea: patterns influenced by seasons, upwelling, and
717 oxygen concentrations. *Progress in Oceanography*, 65(2-4):214–239, 2005.
- 718 Patnaik Sreenivas, KVKRK Patnaik, and KVSR Prasad. Monthly variability of mixed layer over arabian sea using
719 argo data. *Marine Geodesy*, 31(1):17–38, 2008.
- 720 R Subrahmanyam. Studies on the phytoplankton of the west coast of india: Part ii. physical and chemical factors
721 influencing the production of phytoplankton, with remarks on the cycle of nutrients and on the relationship of
722 the phosphate-content to fish landings. In *Proceedings/Indian Academy of Sciences*, volume 50, pages 189–252.
723 Springer, 1959.
- 724 R Subrahmanyam and AH Sarma. Studies on the phytoplankton of the west coast of india. part iii. seasonal variation
725 of the phytoplankters and environmental factors. *Indian Journal of Fisheries*, 7(2):307–336, 1960.
- 726 Laura Ursella, Vanessa Cardin, Mirna Batistić, Rade Garić, and Miroslav Gačić. Evidence of zooplankton vertical
727 migration from continuous southern adriatic buoy current-meter records. *Progress in oceanography*, 167:78–96,
728 2018.
- 729 Laura Ursella, Sara Pensieri, Enric Pallàs-Sanz, Sharon Z Herzka, Roberto Bozzano, Miguel Tenreiro, Vanessa Cardin,
730 Julio Candela, and Julio Sheinbaum. Diel, lunar and seasonal vertical migration in the deep western gulf of mexico
731 evidenced from a long-term data series of acoustic backscatter. *Progress in Oceanography*, 195:102562, 2021.
- 732 V Vijith, PN Vinayachandran, V Thushara, P Amol, D Shankar, and AC Anil. Consequences of inhibition of mixed-
733 layer deepening by the west india coastal current for winter phytoplankton bloom in the northeastern arabian sea.
734 *Journal of Geophysical Research: Oceans*, 121(9):6583–6603, 2016.
- 735 V Vijith, SR Shetye, AD Gouveia, SSC Shenoi, GS Michael, and D Sundar. Circulation in the region of the west
736 india coastal current in march 1994 hydrographic and altimeter data. *Journal of Earth System Science*, 131(1):
737 16, 2022.

- 738 Peter H Wiebe, Charles H Greene, Timothy K Stanton, and Janusz Burczynski. Sound scattering by live zooplankton
739 and micronekton: empirical studies with a dual-beam acoustical system. *The Journal of the Acoustical Society of*
740 *America*, 88(5):2346–2360, 1990.
- 741 Jerry D Wiggert, RR Hood, Karl Banse, and JC Kindle. Monsoon-driven biogeochemical processes in the arabian
742 sea. *Progress in Oceanography*, 65(2-4):176–213, 2005.
- 743 Monika Winder and Daniel E Schindler. Climatic effects on the phenology of lake processes. *Global change biology*,
744 10(11):1844–1856, 2004.
- 745 Karen F Wishner, Marcia M Gowing, and Celia Gelfman. Mesozooplankton biomass in the upper 1000 m in the
746 arabian sea: overall seasonal and geographic patterns, and relationship to oxygen gradients. *Deep Sea Research*
747 *Part II: Topical Studies in Oceanography*, 45(10-11):2405–2432, 1998.

Table 1: ADCP deployment details at the locations. The temporal resolution is 1 hour, bin size(vertical resolution) 4 m. All ADCPs are operated at 153.3 kHz. The moorings are at a water column depth of 950–1200 m on the continental slope and are serviced on yearly basis according to ship availability. The 6th column consists of Reference echo intensity (Er) for each beam, while the 7th column contains the corresponding RSSI conversion factor [Deines, 1999].

Station (Position; °E, °N)	Date		Depth			
	Deployment	Recovery	Ocean	ADCP	Er	Kc
Okha (67.47, 22.26)	01/10/2018	01/12/2019	996	118	37 , 37 , 37 , 36	0.42 , 0.44 , 0.42 , 0.43
	01/12/2019	04/12/2020	1166	312	39 , 36 , 38 , 36	0.42 , 0.44 , 0.42 , 0.43
	04/12/2020	08/03/2022	1021	144	41 , 37 , 38 , 37	0.42 , 0.44 , 0.42 , 0.43
	08/03/2022	01/01/2023	1019	142	37 , 38 , 39 , 36	0.42 , 0.44 , 0.42 , 0.43
Mumbai (69.24, 20.01)	09/11/2017	29/09/2018	1025	150	36 , 34 , 39 , 42	0.40 , 0.40 , 0.40 , 0.40
	29/09/2018	29/11/2019	1122	125	35 , 36 , 39 , 42	0.40 , 0.40 , 0.40 , 0.40
	29/11/2019	02/12/2020	1143	164	37 , 34 , 39 , 43	0.40 , 0.40 , 0.40 , 0.40
	02/12/2020	06/03/2022	1125	142	36 , 34 , 39 , 42	0.40 , 0.40 , 0.40 , 0.40
	07/03/2022	02/01/2023	1103	158	37 , 34 , 40 , 43	0.40 , 0.40 , 0.40 , 0.40
Jaigarh (71.12, 17.53)	27/10/2017	27/09/2018	1039	198	32 , 35 , 33 , 32	0.45 , 0.45 , 0.45 , 0.45
	27/09/2018	30/10/2019	1032	164	32 , 35 , 33 , 31	0.45 , 0.45 , 0.45 , 0.45
	03/11/2019	30/11/2020	1142	264	32 , 36 , 33 , 32	0.45 , 0.45 , 0.45 , 0.45
	30/11/2020	05/03/2022	1099	119	33 , 36 , 34 , 32	0.45 , 0.45 , 0.45 , 0.45
Goa (72.74, 15.17)	03/10/2017	25/09/2018	1000	174	35 , 37 , 34 , 35	0.44 , 0.44 , 0.40 , 0.41
	25/09/2018	16/10/2019	969	145	38 , 36 , 36 , 34	0.44 , 0.44 , 0.40 , 0.41
	16/10/2019	29/11/2020	966	143	44 , 38 , 36 , 43	0.44 , 0.44 , 0.40 , 0.41
	29/11/2020	03/03/2022	985	157	35 , 40 , 35 , 38	0.44 , 0.44 , 0.40 , 0.41
	03/03/2022	05/01/2023	984	159	35 , 38 , 35 , 34	0.44 , 0.44 , 0.40 , 0.41
Udupi (74.04, 12.5)	05/10/2017	06/10/2018	1028	176	44 , 46 , 29 , 35	0.45 , 0.45 , 0.45 , 0.45
	06/10/2018	18/10/2019	1027	179	32 , 38 , 30 , 36	0.45 , 0.45 , 0.45 , 0.45
	18/10/2019	11/12/2020	1018	168	33 , 37 , 31 , 38	0.45 , 0.45 , 0.45 , 0.45
	11/03/2022	06/01/2023	1036	155	31 , 32 , 32 , 33	0.45 , 0.45 , 0.45 , 0.45
Kollam (75.44, 9.05)	07/10/2017	08/10/2018	1174	200	43 , 55 , 45 , 43	0.49 , 0.50 , 0.49 , 0.50
	08/10/2018	20/10/2019	1160	123	49 , 62 , 46 , 46	0.49 , 0.50 , 0.49 , 0.50
	20/10/2019	13/12/2020	1209	176	52 , 61 , 54 , 55	0.49 , 0.50 , 0.49 , 0.50
	13/12/2020	13/03/2022	1129	91	49 , 51 , 46 , 47	0.49 , 0.50 , 0.49 , 0.50
	13/03/2022	08/01/2023	1149	164	41 , 48 , 43 , 41	0.49 , 0.50 , 0.49 , 0.50
Kanyakumari (77.39, 6.96)	16/11/2016	08/10/2017	1096	252	37 , 36 , 37 , 37	0.42 , 0.44 , 0.42 , 0.43
	08/10/2017	10/10/2018	1055	181	32 , 34 , 38 , 35	0.45 , 0.45 , 0.45 , 0.45
	10/10/2018	22/10/2019	1075	180	36 , 34 , 39 , 36	0.45 , 0.45 , 0.45 , 0.45
	22/10/2019	14/12/2020	1060	167	33 , 35 , 36 , 35	0.45 , 0.45 , 0.45 , 0.45
	14/12/2020	14/03/2022	1184	287	34 , 36 , 36 , 35	0.45 , 0.45 , 0.45 , 0.45

Table 2:

Volumetric samples of zooplankton of various stations. The sampling depth range is standardised for later years for bin range of 0–25m, 25–50m, 50–75m, 75–100m, 100–150m. The abbreviations are in the following manner: Okha (O), Mumbai (M), Jaigarh (J), Goa (G), Udupi (U), Kollam (K), Kanyakumari (KK); The number tags corresponds to particular cruise of a station.

Sample number	Tag	Lat($^{\circ}$ N)	Lon($^{\circ}$ E)	Date	Time (IST)	Sampling depth range (m)
1-3	G1	15.18	72.79	25 Sep 18	452	50–25, 100–50, 150–100
4-6	G2	15.16	72.71	25 Sep 18	2108	50–25, 100–50, 150–100
7-10	G2	15.16	72.71	25 Sep 18	2137	40–20, 60–40, 80–60, 100–80
11-14	J1			26 Sep 18	2000	40–20, 60–40, 80–60, 100–80
15-17	J2			27 Sep 18	2000	50–25, 100–50, 150–100
18-21	J2			27 Sep 18	2100	40–20, 60–40, 80–60, 100–80
22-25	M1	20	69.19	28 Sep 18	2135	40–20, 60–40, 80–60, 100–80
26-27	M1	20	69.19	28 Sep 18	2205	50–25, 100–50
28-29	M2	20.01	69.2	29 Sep 18	2035	50–25, 100–50
30-33	M2	20.01	69.2	29 Sep 18	2057	40–20, 60–40, 80–60, 100–80
34-37	U1			5 Oct 18	2000	40–20, 60–40, 80–60, 100–80
38-40	U1			5 Oct 18	2100	50–25, 100–50, 150–100
41-43	U2			6 Oct 18	2000	50–25, 100–50, 150–100
44-47	U2			6 Oct 18	2100	40–20, 60–40, 80–60, 100–80
48-51	K1	9.06	75.42	8 Oct 18	421	40–20, 60–40, 80–60, 100–80
52-54	K1	9.06	75.42	8 Oct 18	449	50–25, 100–50, 150–100
55-56	K2	9.04	75.4	8 Oct 18	2027	50–25, 100–50
57-60	K2	9.04	75.4	8 Oct 18	2045	40–20, 60–40, 80–60, 100–80
61-64	G2	15.16	72.74	16 Oct 19	829	50–25, 75–50, 100–75, 150–100
65-67	G3	15.16	72.74	16 Oct 19	1812	50–25, 75–50, 100–75
68-70	K2	9.02	75.42	20 Oct 19	840	50–25, 75–50, 100–75
71-74	K3	9.04	75.43	20 Oct 19	1934	50–25, 75–50, 100–75, 150–100
75-78	KK1			22 Oct 19	742	50–25, 75–50, 100–75, 150–100
79-82	KK2			22 Oct 19	1925	50–25, 75–50, 100–75, 150–100
83-86	J1			30 Oct 19	324	50–25, 75–50, 100–75, 150–100
87-89	J2			4 Nov 19	946	75–50, 100–75, 150–100
90-92	M2	19.98	69.22	29 Nov 19	1434	50–25, 75–50, 100–75
93-96	M3	20.01	69.23	30 Nov 19	958	50–25, 75–50, 100–75, 150–100
97-100	O1	22.24	67.49	1 Dec 19	937	50–25, 75–50, 100–75, 150–100
101	O2	22.25	67.46	1 Dec 19	1957	150–100
102-105	G3	15.68	73.22	28 Nov 20	930	50–25, 75–50, 100–75, 150–100
105-108	G4	15.32	73.22	29 Nov 20	1558	50–25, 75–50, 100–75, 150–100
108-110	J2	17.85	71.21	30 Nov 20	1458	75–50, 100–75, 150–100
111-114	J3	17.91	71.21	1 Dec 20	1052	50–25, 75–50, 100–75, 150–100
115-118	M4	20.03	69.38	2 Dec 20	2016	50–25, 75–50, 100–75, 150–100
119-00	O2	22.41	67.8	4 Dec 20	953	150–100
120-123	O3	22.41	67.79	4 Dec 20	2011	50–25, 75–50, 100–75, 150–100
124-127	K3	9.11	75.72	12 Dec 20	2335	50–25, 75–50, 100–75, 150–100
128-131	K4	9.06	75.74	13 Dec 20	1507	50–25, 75–50, 100–75, 150–100
132-134	KK1	7.62	77.63	14 Dec 20	1226	50–25, 75–50
135-138	KK2	7.62	77.63	14 Dec 20	2047	50–25, 75–50, 100–75, 150–100
139-142	G4	15.32	73.21	3 Mar 22	823	50–25, 75–50, 100–75, 150–100
143-146	G5	15.68	73.21	4 Mar 22	1030	50–25, 75–50, 100–75, 150–100
147-150	M5	19.99	69.23	7 Mar 22	957	50–25, 75–50, 100–75, 150–100
151-154	O3	22.24	67.5	8 Mar 22	806	50–25, 75–50, 100–75, 150–100
155-158	U3	12.5	74.04	12 Mar 22	1156	50–25, 75–50, 100–75, 150–100
159-160	K4	9.04	75.42	13 Mar 22	1027	50–25, 75–50, 100–75
161-164	KK3	6.97	77.4	15 Mar 22	1220	50–25, 75–50, 100–75, 150–100

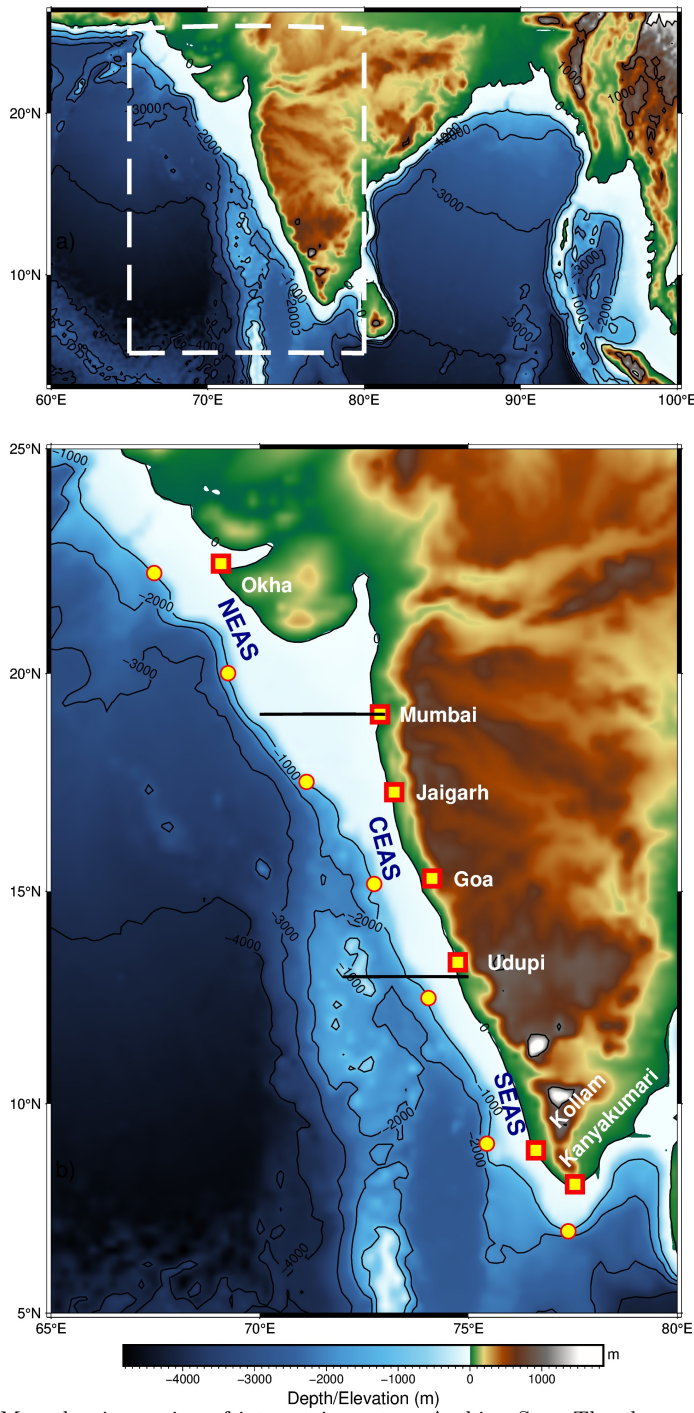


Figure 1: Map showing region of interest in eastern Arabian Sea. The slope moorings are deployed at ~ 1000 m depth as shown in the bathymetry contour. Note the increase in shelf width as we go poleward along the coast. The mooring sites off Okha and Mumbai are in Northern EAS; Jaigarh and Goa in Central EAS while Kollam and Kanyakumari are at Southern EAS. Udupi is situated at the transition zone of Central and Southern EAS.

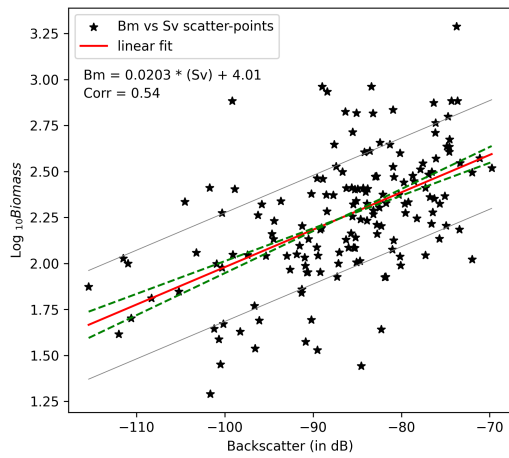


Figure 2: The linear fit line of Biomass (\log_{10} scale) and backscattering strength (in dB). The linear fit line is within the error range of previous result of [Aparna et al., 2022] (contained 67 data points) onto which latest zooplankton volumetric sample data (159 data points) is appended. The regression equation is $y = (0.02 \pm 0.0025) x + (4.0144 \pm 0.2198)$ and correlation value of 0.54. The dashed green lines denote error range of plausible slope and intercept. From the linear equation, the upper and lower bound of error limit leads to an error bar of $\sim 14 \text{ mg m}^{-3}$. The first standard deviation of $\log_{10}(\text{Biomass})$ is ± 0.49 , which results in the backscatter range of 48.58 dB encompassing the entire backscatter range. It signifies the robustness of zooplankton biomass dependency on ADCP measured backscattering strength.

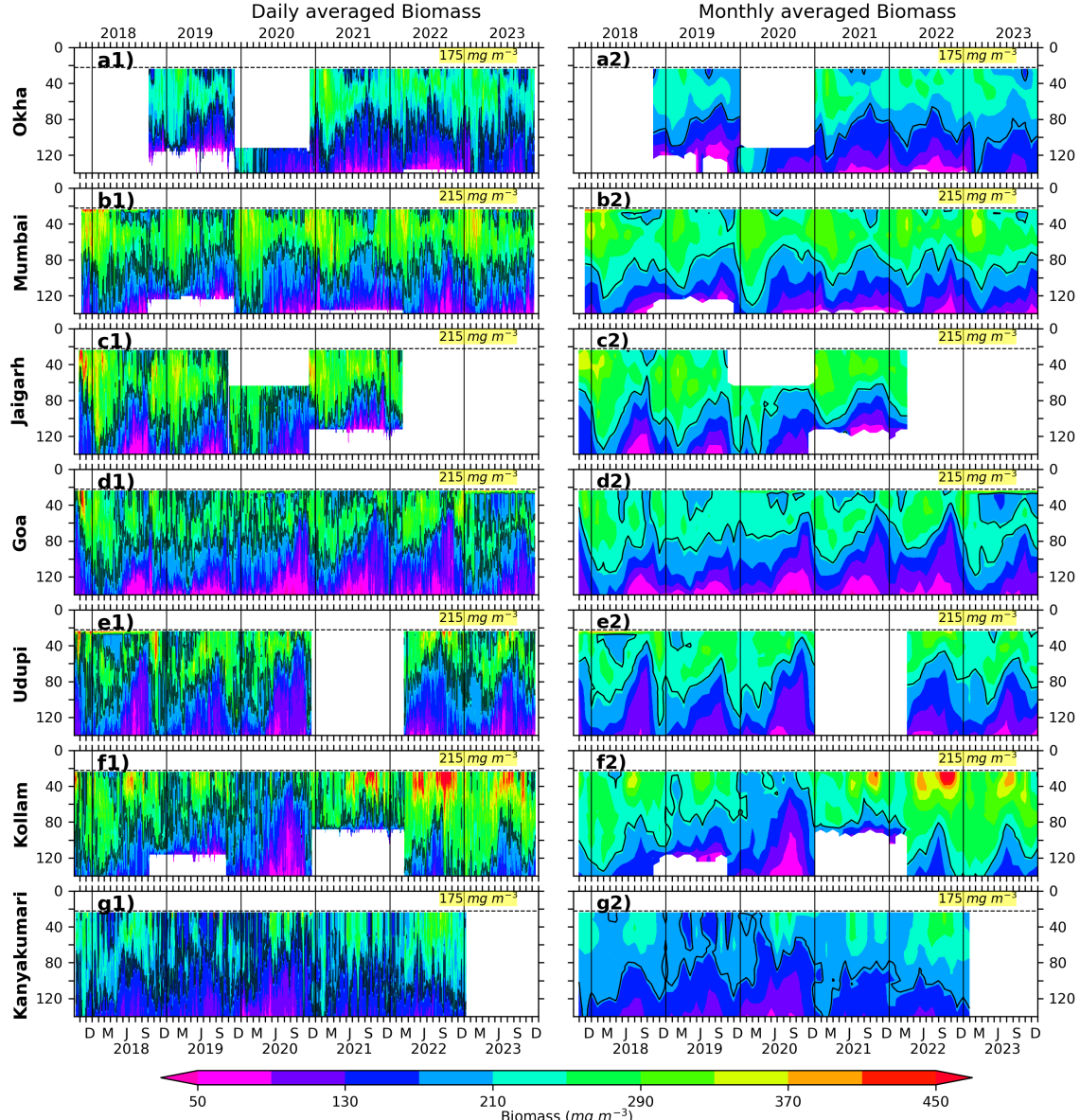


Figure 3: The Daily and monthly averaged biomass for EAS moorings, north (top) to south (bottom). The black contours are marking of 175 mg m^{-3} biomass for Okha and Kanyakumari; 215 mg m^{-3} for Mumbai, Goa and Kollam. The biomass contours are distinct and different based on the physico-chemical parameters and the one that best explains seasonality at respective location. The top 10% of data is discarded due to echo noise. The dashed line at 22 m marks the top-depth of first bin i.e, 24 m.

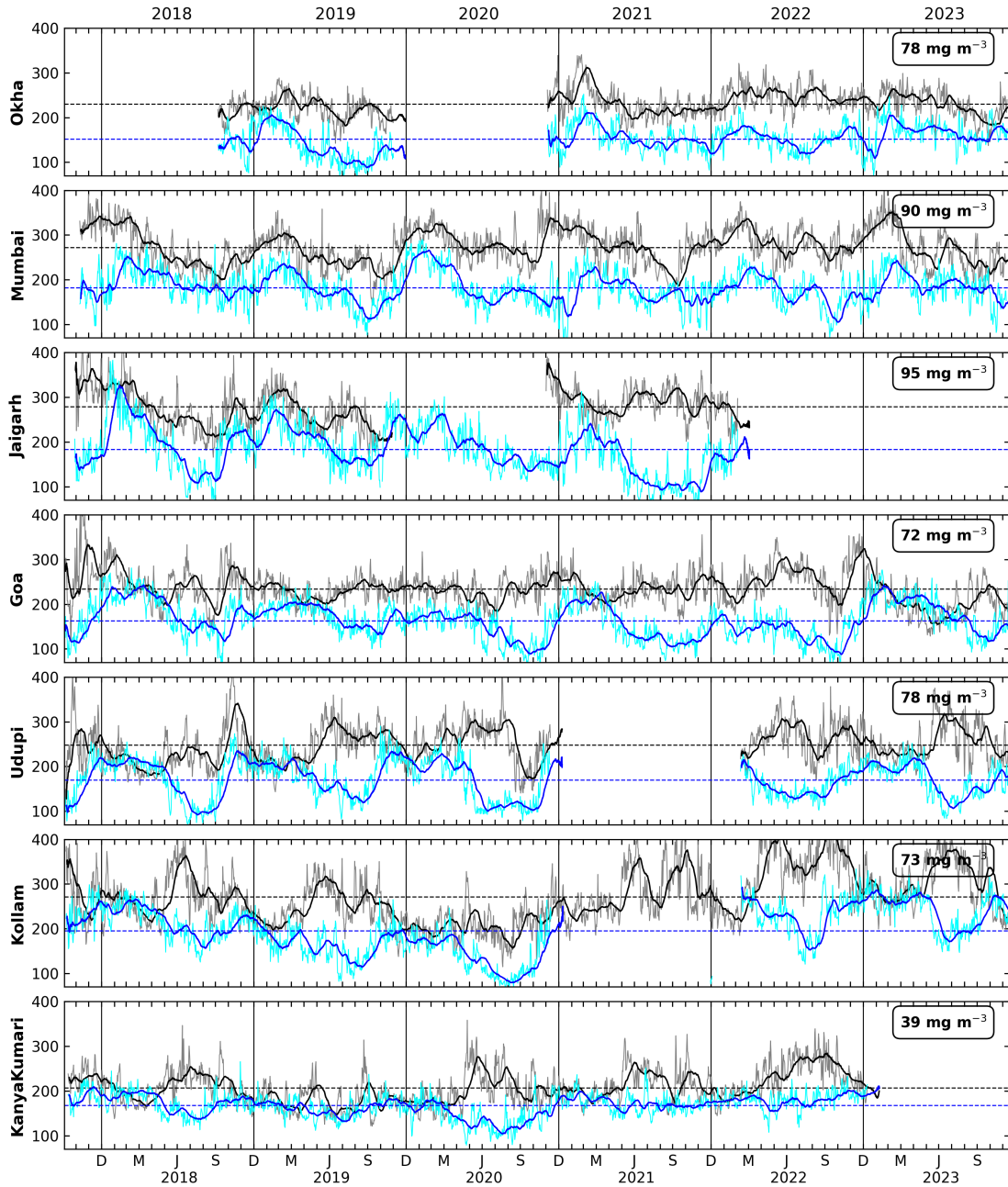


Figure 4: The daily biomass at depth of 40 m and 104 m for all locations shown by grey and cyan curves. The black and blue lines show the 30 day rolling averaged biomass at 40 and 104 m, respectively. The difference in mean biomass at 40 and 104 is shown in top right box. Notice the spikes (bursts) seen in the daily (rolling mean) data of biomass at 40 m that lasts few days (few days to weeks), e.g., during many isolated days of June of 2020 (during entire June–July of 2020). These spikes and bursts are seen at all locations and both at 40 and 104 m, albeit with a varied magnitude.

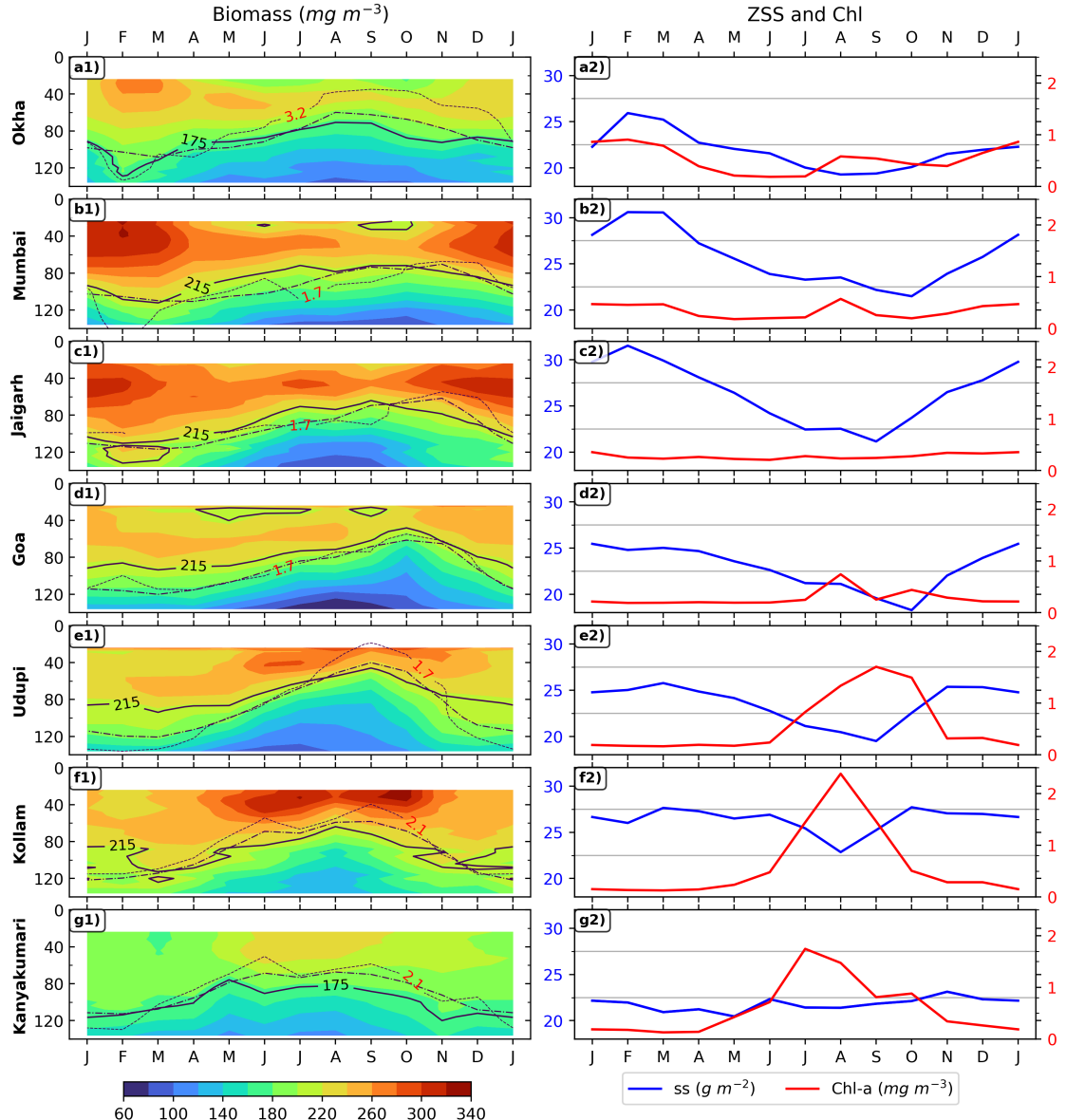


Figure 5: Monthly climatology of zooplankton biomass is shown in left panels for 7 locations, (top to bottom is southward). The D175 and D215 are shown in solid lines; dashed line represents the depth of 23 C isotherm; oxygen contours are shown in dotted lines and labeled for each mooring. The right set of panel plots is showing ZSS (24–140 biomass integral) and chl-a climatology for corresponding locations.

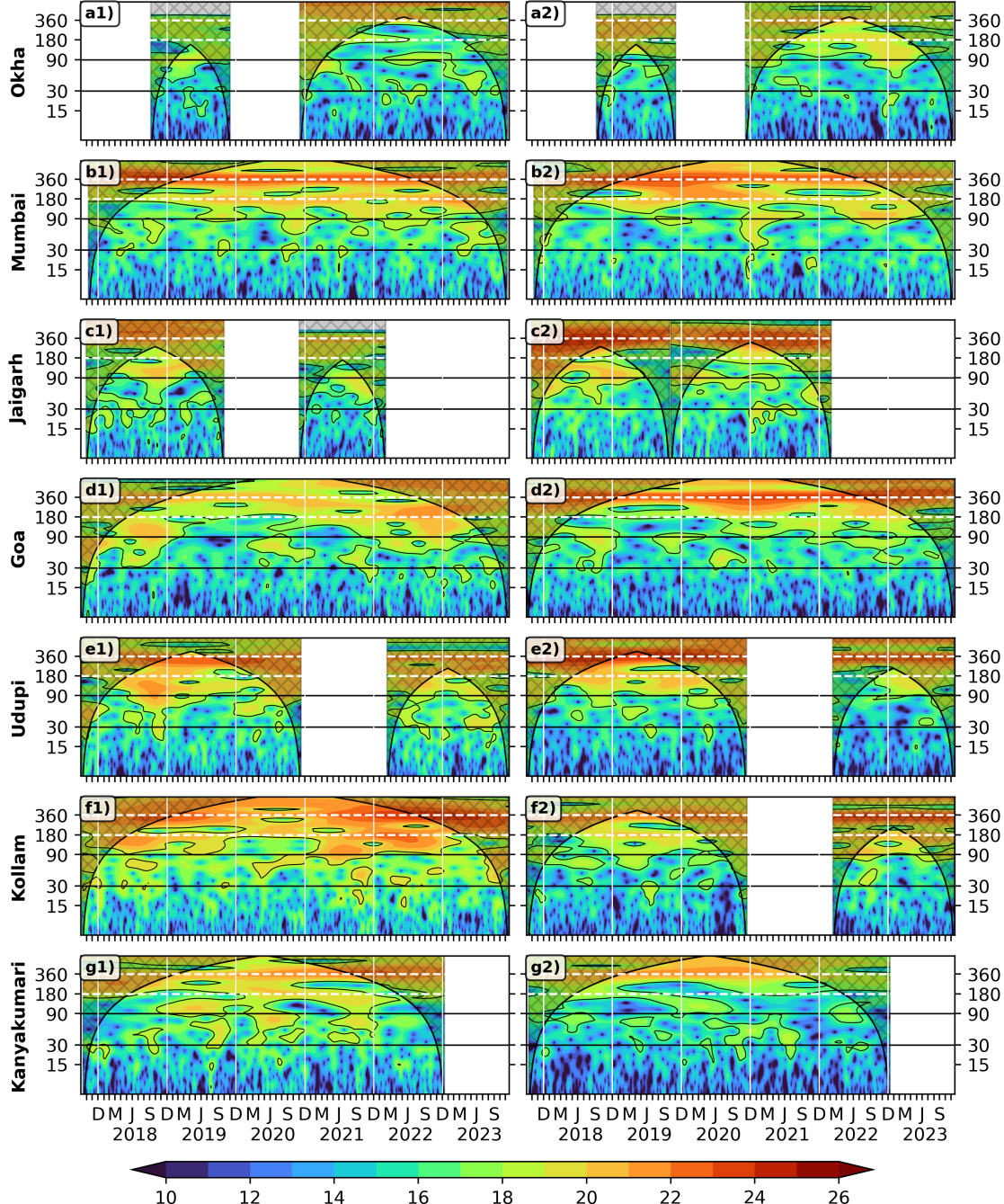


Figure 6: Wavelet power spectra (Morlet) of the 40 m (left panel) and 104 m (right panel) zooplankton biomass plotted against time as abscissa and period in days as ordinate. The wavelet power is in \log_2 scale, the 95% significance is marked in black contours; the cross-shaded region falls under cone of influence. The horizontal dashed white (solid black) lines shows annual and semi-annual periods (intraseasonal band). Vertical white lines separates years.

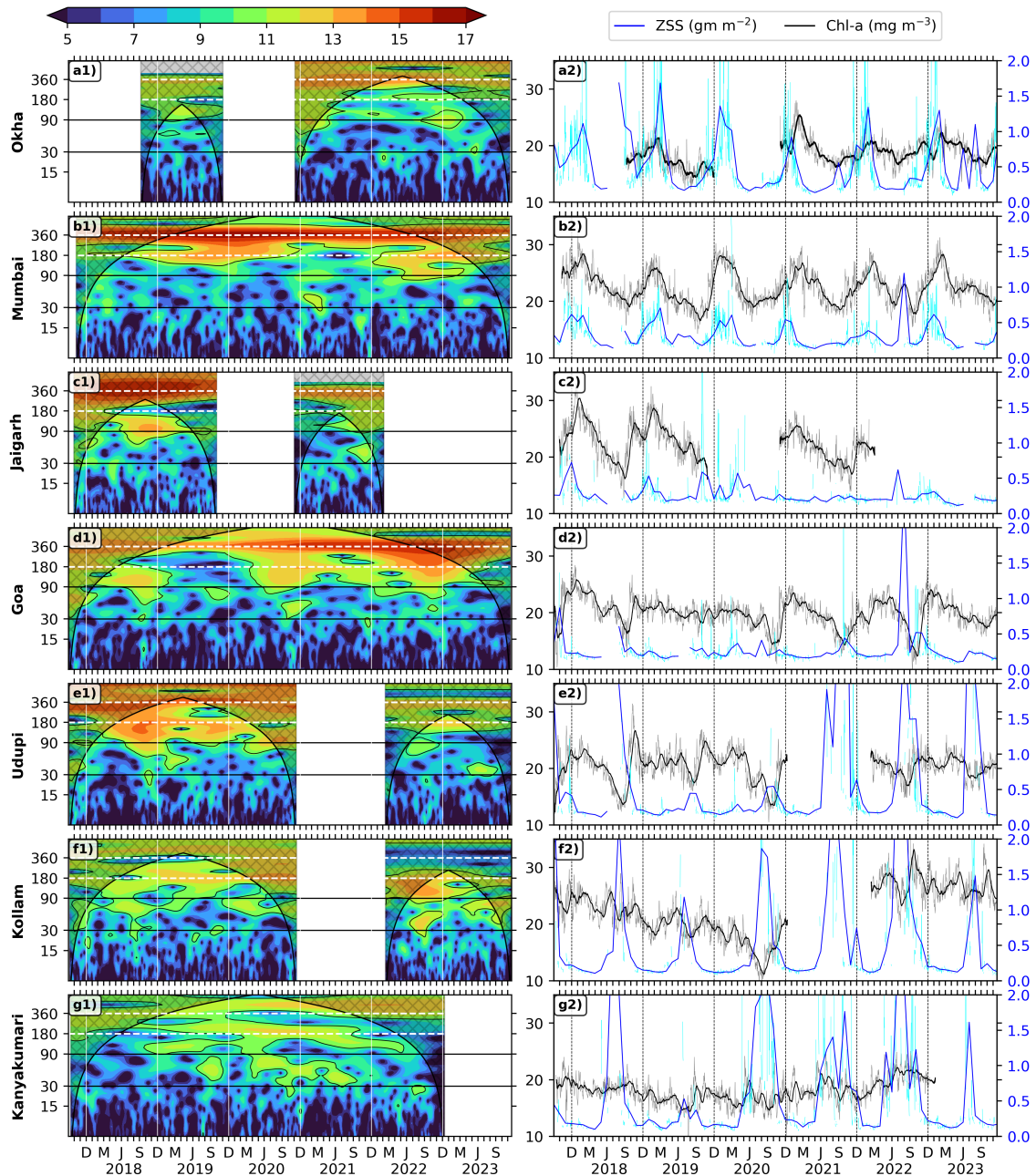


Figure 7: Wavelet power spectra (Morlet) of zooplankton standing stock plotted against time as abscissa and period in days as ordinate. The wavelet power is in \log_2 scale, the 95% significance is marked in black contours; The vertical white lines separates years. The right side panel shows the ZSS (24–120 m biomass integral) time series of 30 day rolling mean data (black) overlaid upon daily data (Grey). The 30 day rolling mean data of chl-a (solid blue) is plotted over its daily data (cyan).

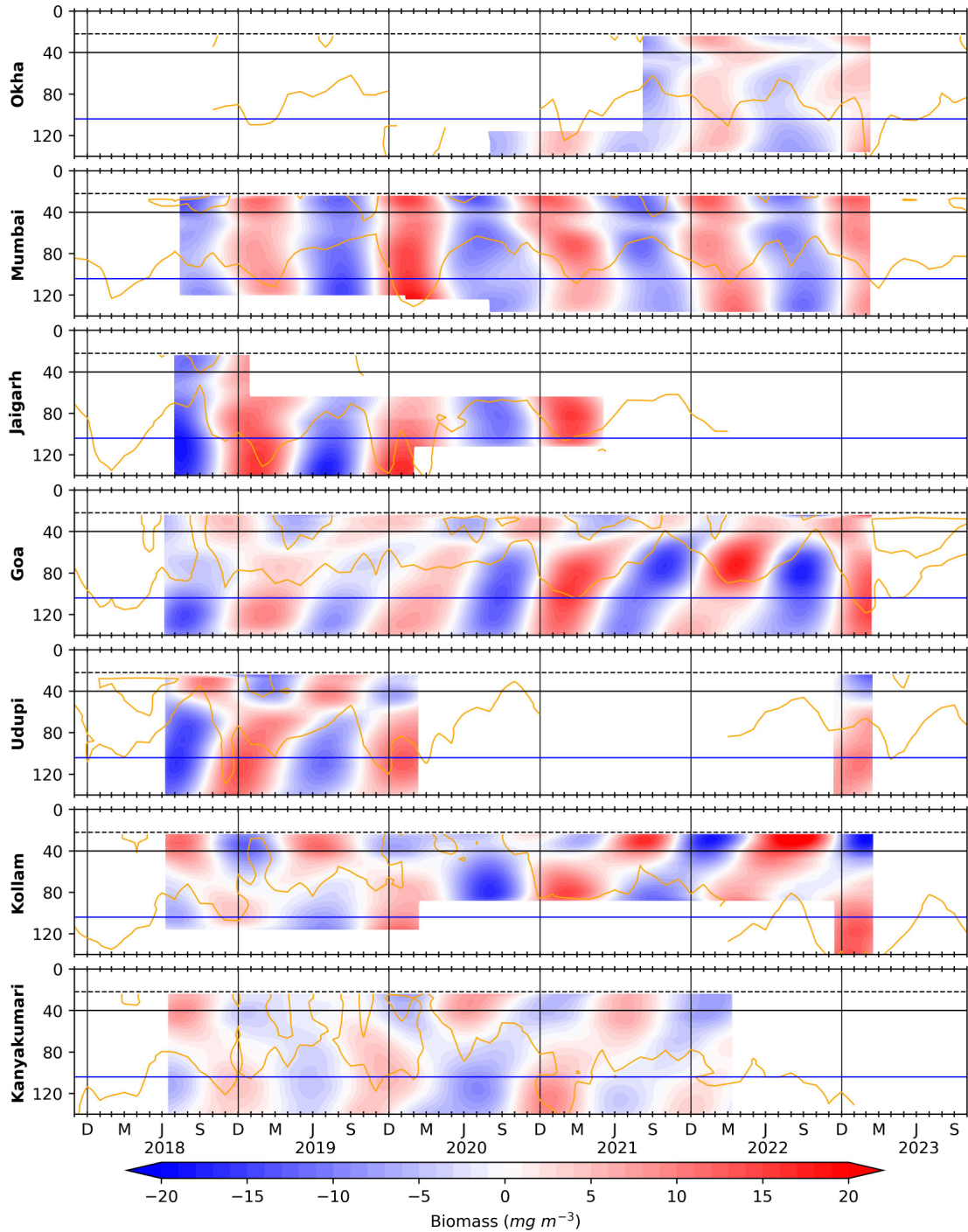


Figure 8: The biomass variation occurring in annual band (300 to 400 days). Owing to the presence of monsoon, there is a variation driven by associated upwelling (downwelling) processes in summer (winter) monsoon. and The horizontal black and blue lines is for 40 and 104 m respectively; vertical black lines separate the years. The dashed line at 22 m marks the top-depth of first bin i.e, 24 m ± 2 solid orange curves denotes D215 (D175 off Okha and Kanyakumari)

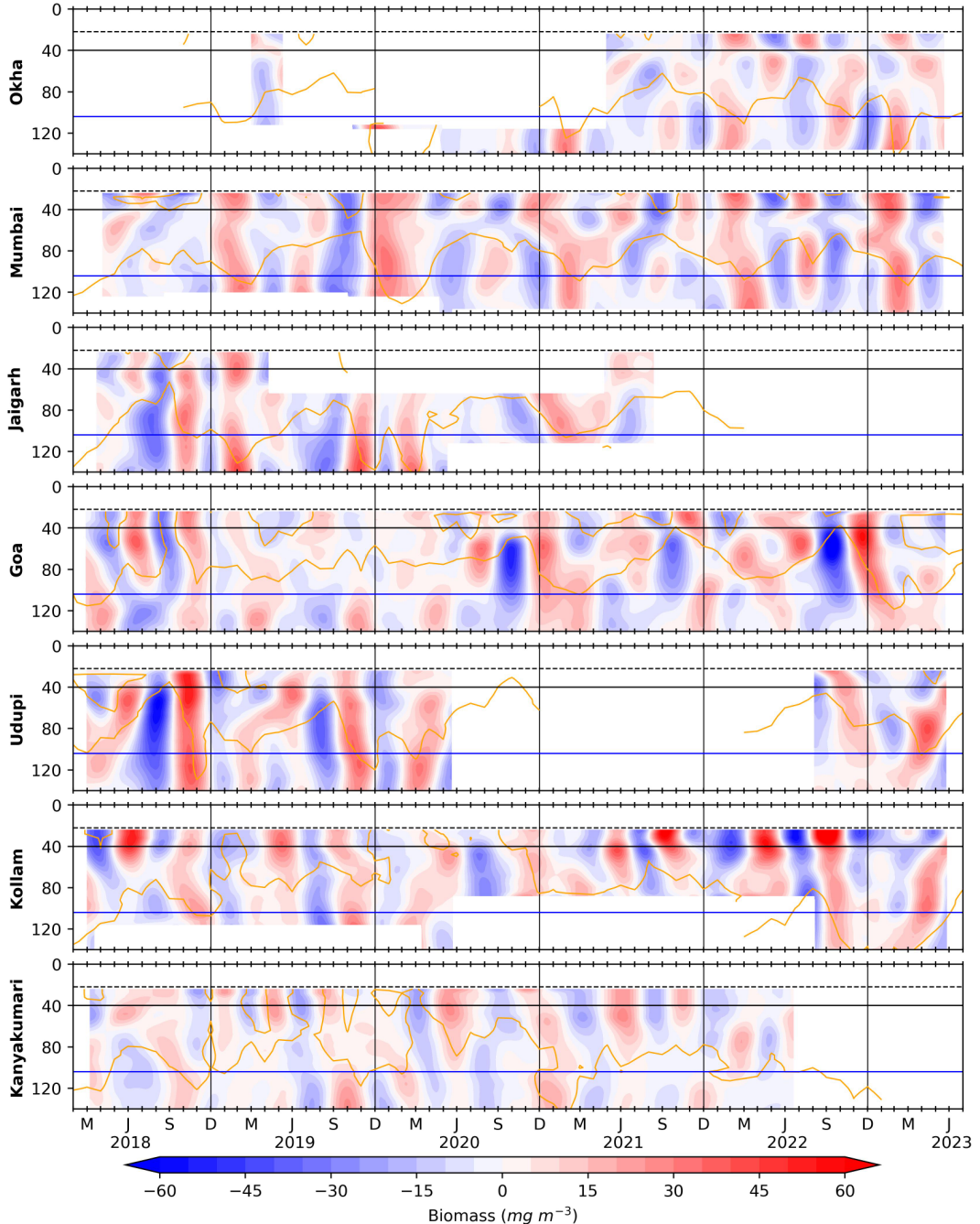


Figure 9: The biomass variation occurring in 100 to 250 days period (between the seasons and within a year record or intra-annual band) is obtained using a band pass filter. The horizontal black and blue lines is for 40 and 104 m respectively; vertical black lines separate the years. The dashed line at 22 m marks the top-depth of first bin i.e, 24 m and solid orange curves denotes D215 (D175 off Okha and Kanyakumari).

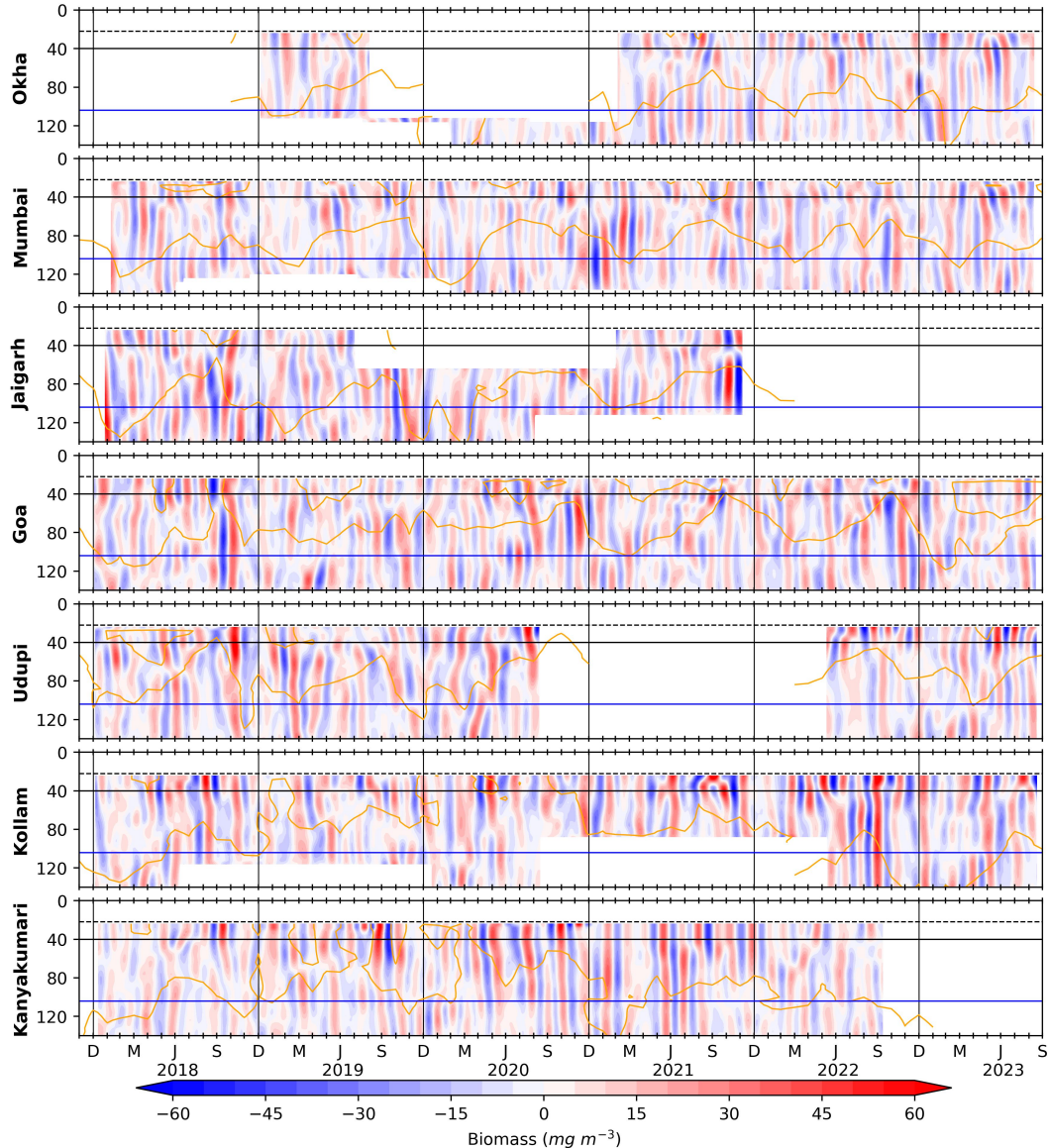


Figure 10: Biomass variation found in the Intraseasonal band i.e., 30 to 90 days period is obtained using a lanczos band pass filter. The horizontal black and blue lines is for 40 and 104 m respectively; vertical black lines separate the years and solid orange curves denotes D215 (D175 off Okha and Kanyakumari). The dashed line at 22 m marks the top-depth of first bin i.e, 24 m. Intraseasonal variability is seen throughout the record, is coherent along the slope and its magnitude is stronger during August to November.

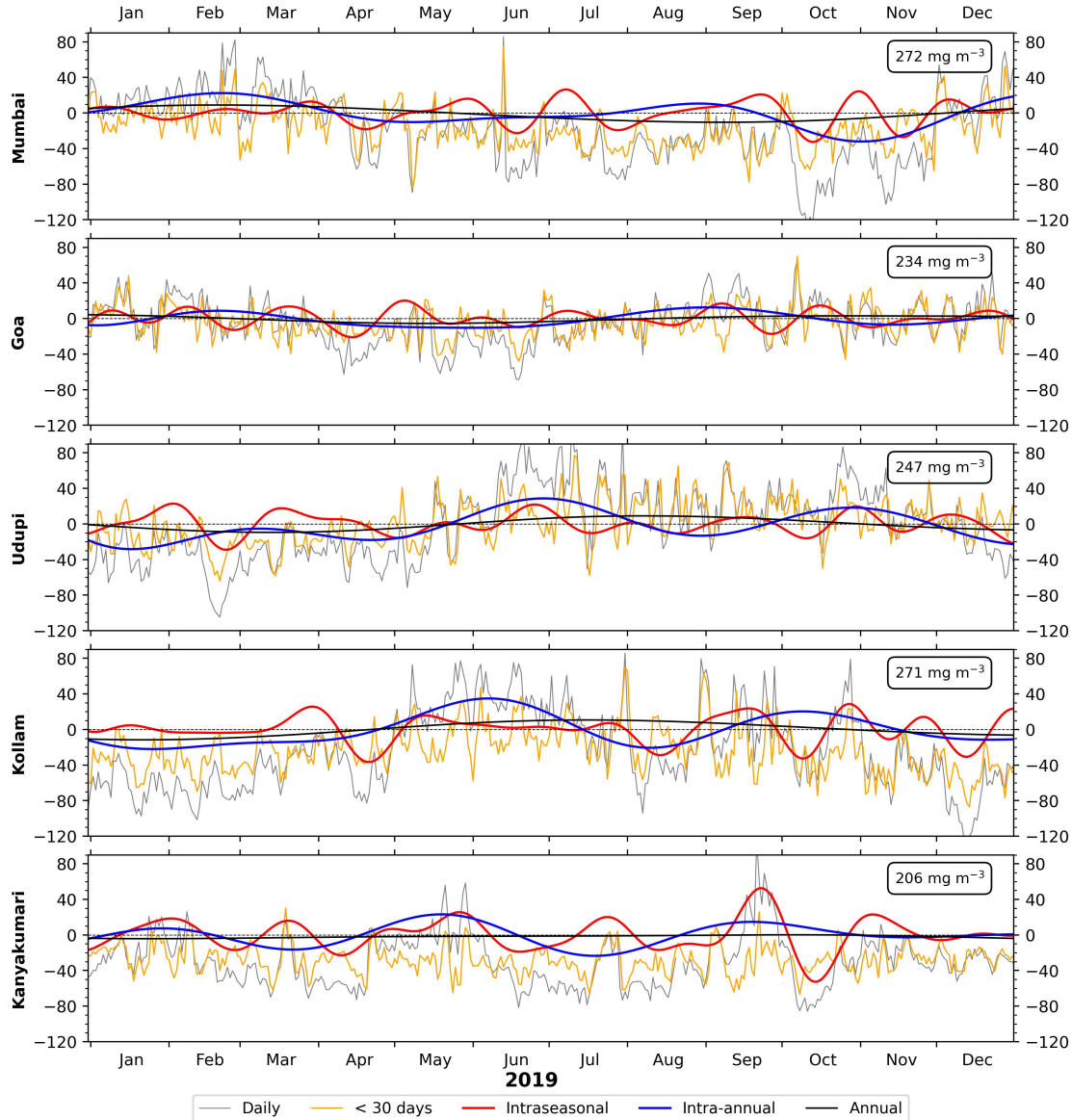


Figure 11: Comparison between mean-removed daily biomass time series at 40 m and the distinct components of variability off Mumbai, Goa and Kollam for 2019. The biomass units are mg m^{-3} and its mean for respective location is shown in top right box. The cyan curve is sum of all low frequency components above 30 days, i.e., annual, intra-annual and 30 to 90 days intraseasonal variability. Off Mumbai and Kollam, an increase in biomass is noticed from May onward and lasting till late monsoon with weeks of low biomass during August due to contribution from each component of variability.